REPORT DOCUMENTATION PAGE

Form Approved
OMB No. 0704-0188

1. REPORT DATE	2. REPORT TYPE	3. DATES COVERED *(From - To)*
12 July 2017	Conference Paper with Briefing Charts	22 May 2017 - 30 July 2017

4. TITLE AND SUBTITLE
Wavelength Modulation Spectroscopy for Temperature and Species Concentration in the Plume of a Supersonic Nozzle (Conference Paper with Briefing Charts)

5a. CONTRACT NUMBER

5b. GRANT NUMBER

5c. PROGRAM ELEMENT NUMBER

6. AUTHOR(S)
Amanda S. Makowiecki, Torrey R. S. Hayden, Michael R. Nakles, Nickolas Pilgram, Natalia A. MacDonald, William A. Hargus, and Gregory B. Rieker

5d. PROJECT NUMBER

5e. TASK NUMBER

5f. WORK UNIT NUMBER
Q1U0

7. PERFORMING ORGANIZATION NAME(S) AND ADDRESS(ES)
Air Force Research Laboratory (AFMC)
AFRL/RQRC
10 E. Saturn Blvd.
Edwards AFB, CA 93524-7680

8. PERFORMING ORGANIZATION REPORT NUMBER

9. SPONSORING/MONITORING AGENCY NAME(S) AND ADDRESS(ES)
Air Force Research Laboratory (AFMC)
AFRL/RQR
5 Pollux Drive
Edwards AFB, CA 93524-7048

10. SPONSOR/MONITOR'S ACRONYM(S)

11. SPONSOR/MONITOR'S REPORT NUMBER(S)
AFRL-RQ-ED-TP-2017-143

12. DISTRIBUTION/AVAILABILITY STATEMENT
Approved for Public Release; Distribution Unlimited. PA Clearance Number: 17393 Clearance Date: 19 June 2017 - TP
Approved for Public Release; Distribution Unlimited. PA Clearance Number: 17443 Clearance Date: 11 July 2017 - BC/VG
Accompanying Briefing Charts AFRL-RQ-ED-VG-2017-166

13. SUPPLEMENTARY NOTES
For presentation at 53rd AIAA Joint Propulsion Conference; Atlanta, GA, USA; 10-12 July 2017
Prepared in collaboration with University of Colorado and ERC Inc. The U.S. Government is joint author of the work and has the right to use, modify, reproduce, release, perform, display, or disclose the work. Conference Paper with Briefing Charts

14. ABSTRACT
We measure the plume temperature and species concentration profiles of a heated mixture of ammonia and steam flowing through a miniature converging-diverging nozzle (area ratio 5:1, exit diameter 4.57 mm). The nozzle operating conditions are intended to simulate the plume of a thruster system operating in vacuum environments. Wavelength modulation spectroscopy (WMS) is a laser absorption spectroscopy technique that allows for quantitative, time-resolved, sensitive diagnostics of gaseous flows. The goal of the measurements is to assess the potential of WMS as a diagnostic technique for characterizing this type of system. The measurements use three multiplexed fiber-coupled tunable diode lasers: two for measuring temperature and H2O concentration and one for measuring NH3 concentration. The multiplexed laser beam is spatially translated across the plume on a two-axis stage. Using Abel transforms, we are able to successfully resolve the structure of the under-expanded plume despite absorption signals as low as 9e-4. As a result, WMS demonstrates excellent promise as a sensitive diagnostic tool for resolving the profile of such plumes.

15. SUBJECT TERMS

16. SECURITY CLASSIFICATION OF:			17. LIMITATION OF ABSTRACT	18. NUMBER OF PAGES	19a. NAME OF RESPONSIBLE PERSON
a. REPORT	b. ABSTRACT	c. THIS PAGE			William Hargus
Unclassified	Unclassified	Unclassified	SAR	64	19b. TELEPHONE NUMBER *(Include area code)* N/A

Wavelength Modulation Spectroscopy for Temperature and Species Concentration in the Plume of a Supersonic Nozzle

Amanda S. Makowiecki[1], Torrey R. S. Hayden[1], Michael R. Nakles[2], Nickolas Pilgram[2], Natalia A. MacDonald[3], William A. Hargus[4], and Gregory B. Rieker[5]

We measure the plume temperature and species concentration profiles of a heated mixture of ammonia and steam flowing through a miniature converging-diverging nozzle (area ratio 5:1, exit diameter 4.57 mm). The nozzle operating conditions are intended to simulate the plume of a thruster system operating in vacuum environments. Wavelength modulation spectroscopy (WMS) is a laser absorption spectroscopy technique that allows for quantitative, time-resolved, sensitive diagnostics of gaseous flows. The goal of the measurements is to assess the potential of WMS as a diagnostic technique for characterizing this type of system. The measurements use three multiplexed fiber-coupled tunable diode lasers: two for measuring temperature and H_2O concentration and one for measuring NH_3 concentration. The multiplexed laser beam is spatially translated across the plume on a two-axis stage. Using Abel transforms, we are able to successfully resolve the structure of the under-expanded plume despite absorption signals as low as 9e-4. As a result, WMS demonstrates excellent promise as a sensitive diagnostic tool for resolving the profile of such plumes.

Nomenclature

A_λ	=	path averaged absorbance area of feature at wavelength, λ
χ_i	=	mole fraction of species, *i*
I_0	=	incident intensity on gas sample
I_t	=	transmitted intensity out of gas sample
L	=	pathlength probed by laser sensor
λ	=	wavelength of light
ν	=	optical frequency of light
$\phi(\lambda)$	=	lineshape function of absorption feature
$S_\lambda(T)$	=	linestrength of absorption feature
T	=	temperature of gas sample
R	=	outer radius of jet
r	=	radial position within jet
y	=	vertical position within jet
X_{2f}	=	X component of lockin amplifier at *2f*
Y_{2f}	=	Y component of lockin amplifier at *2f*
R_{1f}	=	root-sum-square magnitude of the X and Y components of the lock-in outputs at $1f$
A'_λ	=	radial distribution of absorbance area of feature at wavelength, λ

[1] PhD student, Dept. of Mechanical Engineering, University of Colorado, Boulder, CO 80309
[2] Researcher, In-Space Propulsion Branch, ERC Inc, Edwards Air Force Base, CA 93524
[3] Researcher, In-Space Propulsion Branch, Air Force Research Laboratory, Edwards Air Force Base, CA 93524
[4] Program Manager, In-Space Propulsion Branch, Air Force Research Laboratory, Edwards Air Force Base, CA 93524
[5] Assistant Professor, Dept. of Mechanical Engineering, University of Colorado, Boulder, CO 80309

I. Introduction

Plume diagnostics are important tools for characterizing the operation of rockets and other propulsion systems. However, many systems are difficult to probe due to their size (both large and small), high velocities, caustic products, and varying pressure conditions. Laser based diagnostics are ideal for these environments as they are time-resolved, non-intrusive, and can be very sensitive. Time-resolved measurements of species concentration and plume temperature can be used to validate models and quantify the state-of-health of these systems. Wavelength modulation spectroscopy (WMS) is a method of absorption spectroscopy particularly well suited for these measurements because it is quantitative, reduces noise, and has improved sensitivity over traditional tunable diode laser methods [1]-[2].

In absorption spectroscopy, light is passed through a gas sample and will be absorbed if the wavelength of the light is resonant with a molecular transition. For homogenous mixtures, absorbance (α) of the light at a given wavelength (λ), is quantified by Beer's Law (1). Io represents the initial intensity of the light, and It represents the transmitted intensity of the light after it has passed through the sample. From the absorbance, gas properties such as species concentration (Xi), pressure (P), pathlength (L) and temperature (through the linestrength $S_\lambda(T)$) can be calculated, if the lineshape function Φ is known (or if an entire isolated lineshape is measured, since $\int_{-\infty}^{+\infty} \phi(\lambda)d\lambda \equiv 1$). Transition specific parameters such as $S_\lambda(T)$ and Φ are calculated from spectroscopic parameters found in databases such as HITRAN 2012 [3] or from experimental studies [4]–[6].

$$\alpha(\lambda) = S_\lambda(T)PX_iL\phi(\lambda) = -\ln\left(\frac{I_t}{I_o}\right) \quad (1)$$

Tunable diode lasers (TDLs) are commonly used in absorption spectroscopy due to their small size, low cost relative to other laser sources, and robust nature (resulting from of their development by the telecom industry). The wavelength of a TDL tunes approximately linearly with the tuning of the laser injection current, allowing the center wavelength of the TDL to be swept over an absorption feature [7]. WMS is a modification of tunable diode laser absorption spectroscopy where the wavelength of the TDL is rapidly modulated at a frequency f (here, approximately 100 kHz) [2]. In the presence of absorption, this modulation gives rises to harmonics of the original modulation frequency (f) in the detected intensity signal. The second harmonic (2f) is of particular interest, as the magnitude is linearly related to absorbance and can therefore be used to infer thermodynamic properties of the gas. If the second harmonic signal alone is used for thermodynamic measurements, the laser intensity must be calibrated in-situ with a known mixture, which is not possible in many engineering applications due to window fouling, vibrating optics and beam steering. It has been demonstrated that dividing the second harmonic signal by the first harmonic signal removes the dependence on laser intensity, thus eliminating the need for intensity calibrations [1]. The resulting signal is referred to hereafter as the normalized 2f signal. A lock-in amplifier is used to isolate the harmonics, filtering noise outside of the bandwidth of the lock-in amplifier, and shifting the detection to higher frequencies where laser and system noise is decreased. By comparing the shape and magnitude of the normalized 2f signal from the lock-in detector to simulated signals, thermodynamic properties such as pressure, temperature and species concentration can be measured.

II. Experimental Setup

The WMS measurements are performed at the Air Force Research Laboratory at Edwards Air Force Base in California. The converging-diverging nozzle and heating system was mounted inside of chamber 4 within the Spacecraft Propulsion Laboratory. The laser light and translation stage control system signals were passed into chamber 4 via fiber optic and electrical vacuum feedthroughs on the chamber.

The exhaust plume examined in this study is composed of a mixture of anhydrous ammonia and water. The water concentration of the plume is held at approximately 18% water by mass. The gas flow is preheated by two circulation heaters connected in series. Liquid water from a syringe pump, is injected between the two heating stages, exposing it to the preheated ammonia flow. The syringe pump allows the water flow rate to be precisely controlled and varied. The temperature of the tube where the water enters the ammonia flow stream is monitored by a type K thermocouple. To adequately vaporize the water, water is not injected into the system until the tube, at the entry point, reaches a minimum temperature of 100 ºC. To minimize system exposure to the corrosive effects of ammonia, the system is preheated and purged with nitrogen.

Immediately following the second heating stage, the gas mixture flows through the converging-diverging nozzle seen in Figure 1 to create the plume. This nozzle configuration results in an expansion ratio of 5.19 and an exit Mach number of 3.05. By design, this nozzle creates a highly under-expanded plume at the operational background pressures of 550-720 mTorr.

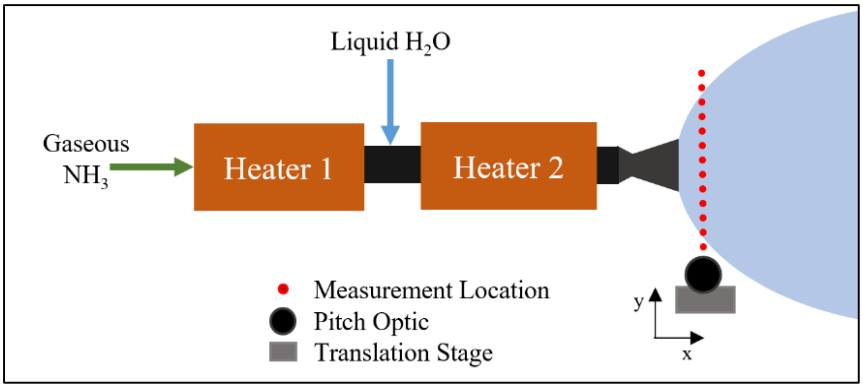

Figure 1: Experimental setup of NH_3 and H_2O injection with translation stage

Three tunable diode lasers are used to probe three distinct absorption features. Laser 1 (Eblana EP1388-DM) and laser 2 (Eblana EP1392-DM) probe H_2O absorption features at 1388 nm and 1392 nm respectively. Laser 3 (Toptica LD-1470-0010-DFB-1) probes an NH_3 feature at 1527nm. The transition at 1388nm reaches a maximum absorption at low temperature, while the transition at 1392nm reaches a maximum absorption at elevated temperatures (approximately 650K). The different temperature dependencies of the H_2O absorption features, results in an absorbance ratio of the two lines that is sensitive to temperature, but also results in low peak absorbance at low temperatures for the feature at 1391.7nm.

A National Instruments PXIe-6368 data acquisition card provides the voltage signal used to modulate the laser injection currents for WMS. The light from the three fiber-coupled lasers is multiplexed onto a single-mode fiber and passed into the vacuum chamber through an optical fiber feed-through, to a launch optic (Thorlabs CFC-5X-C). The beam traverses the plume perpendicular to the flow direction, as shown in Figure 1. The beam is collected by a catch collimator (Oz Optics HPUCO-25-1300/1550-M-25AC-SP) to a 400-micron diameter multimode fiber (Thorlabs M45L01) and passes back through the optical feed-through to an InGaAs photodetector (Thorlabs PDA10CS). The signal from the photodetector is monitored by the PXIe-6368 data acquisition card at a 2MHz sampling rate.

The launch and collection optics are mounted on a 2-axis stage that can be translated in the vertical and horizontal directions through the use of two stepper motors. The translation system enables measurements from -0.4 cm to +0.4 cm relative to the plume center at vertical increments of 0.1 mm, resulting in 81 total measurement locations at 1 mm downstream of the nozzle exit.

III. Data Processing

A. Residual Amplitude Modulation

The magnitude of the absorption signal is linearly correlated with the path length and approximately linearly correlated with pressure, as seen in Equation 1. The small exit diameter of the nozzle (4.57mm) and the low operating pressures within the vacuum chamber (approximately 500 mTorr) resulted in low absorption signals.

$$2f/1f = \sqrt{\left[\left(\frac{X_{2f}}{R_{1f}}\right)_{raw} - \left(\frac{X_{2f}}{R_{1f}}\right)_{bg}\right]^2 + \left[\left(\frac{Y_{2f}}{R_{1f}}\right)_{raw} - \left(\frac{Y_{2f}}{R_{1f}}\right)_{bg}\right]^2} \quad (2)$$

Due to the low pressure and short pathlength, the magnitude of the absorption signal is on the same order of magnitude as the residual amplitude modulation (RAM) of the laser [8], [9]. RAM is caused by non-linear intensity tuning of the laser system that creates harmonic signals even in the absence of absorption (WMS background). It is present in varying degrees in all tuned laser systems. Figure 2 shows the normalized 2f signal of the transmitted intensity (i.e. after absorption) in green and the normalized 2f signal of the incident intensity (i.e. without absorption),

in red. Theoretically, if the laser tuning is exactly linear, the normalized 2f of the incident intensity would be constant at zero.

In Figure 2a it is clear that the non-linear tuning creates a strong background in the normalized 2f signal of the transmitted intensity. The incident intensity is recorded concurrently with the transmitted intensity; this allows the second harmonic components of the non-absorbing incident intensity signal to be subtracted from the second harmonic components of the absorbing transmitted intensity signal according to Equation 2. The parameters X_{2f}, Y_{2f} are the X and Y components of the signals from the digital lockin at 2f. R_{1f} refers to the root mean square of the X and Y parameters at 1f. Finally, the components denoted 'raw' are from the transmitted intensity signal before RAM subtraction, while the components denoted 'bg' or background are from the incident intensity signal. With this procedure, we can isolate the components of the transmitted intensity signal caused by absorption The background-subtracted signal is shown in Figure 2b. This method is applied to all measured signals for all three lasers. The 1392nm feature, shown in Figure 2, is the weakest absorption signal (9E-4 absorbance, or 0.09% absorption), and therefore the most sensitive to the background signal and subtraction.

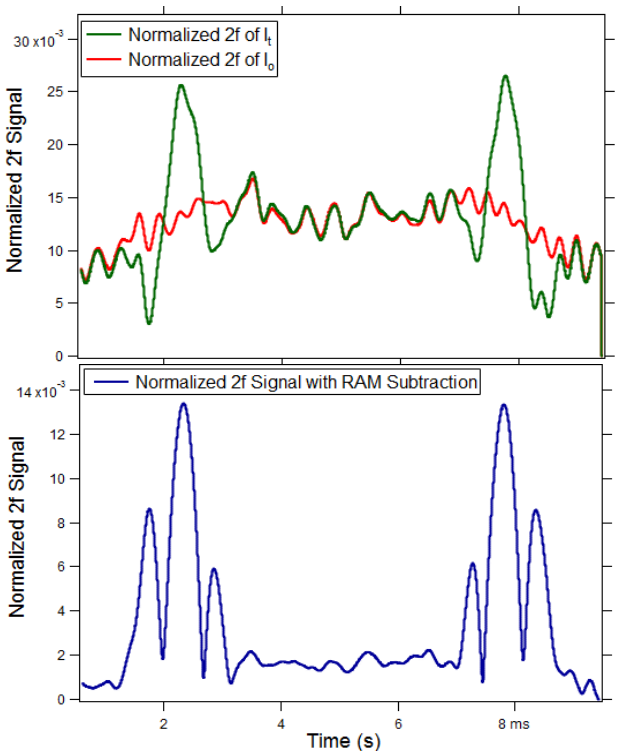

Figure 2: Figure 2a: Normalized 2f signal of transmitted intensity with absorption before RAM subtraction (green), Normalized 2f signal of incident intensity without absorption, showing the RAM contribution (red). Figure 2b: Normalized 2f signal with RAM subtraction.

B. Averaging

For these measurements, we perform scanned-wavelength WMS, where the high frequency wavelength modulation is combined with an additional slow sine wave modulation (100Hz) to scan the average wavelength of the laser across the entire absorption feature [10]. The basic time resolution of the measurement is therefore 200 Hz, as we scan the full normalized 2f signal for each feature twice per cycle of the slow modulation.

Figure 3 shows a single sweep, and a 0.5s average of the normalized 2f signals. Though the single and 0.5s averages are similar for the stronger features probed by lasers 1 and 3, the 0.5s average significantly improves data analysis for the weak 1392nm feature. For the results reported in the remainder of the paper, 0.5s averages are used.

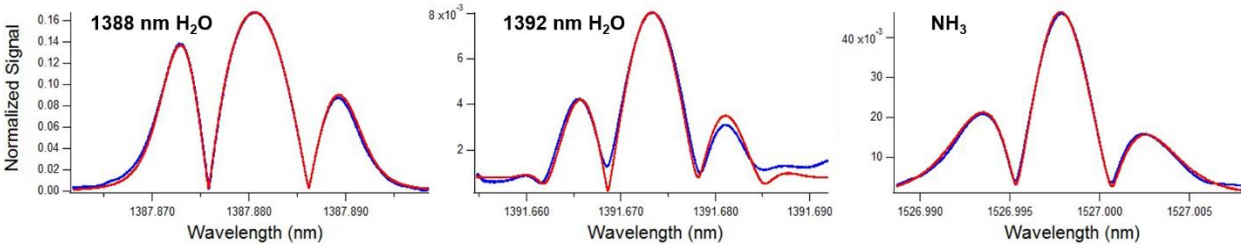

Figure 3: Raw data (red) versus time averaged data (blue) for each absorption feature. Figure 3a: 1388nm H_2O feature, Figure 3b: 1392nm H_2O feature, Figure 3c: NH_3 feature.

C. Absorbance Area

We utilize a fitting procedure similar to that described by [11] to calculate an integrated absorbance area for each absorption feature [6], [3], [5]. Using the integrated absorbance area, rather than the peak normalized 2f signal, simplifies the interpretation of the measured data by removing the dependence of the signal on line broadening. An example of a fit produced with this procedure is shown in Figure 4. The good agreement between the fit and data ensures that the absorbance area calculated by the fit is representative of the absorbance area of the measured absorption feature.

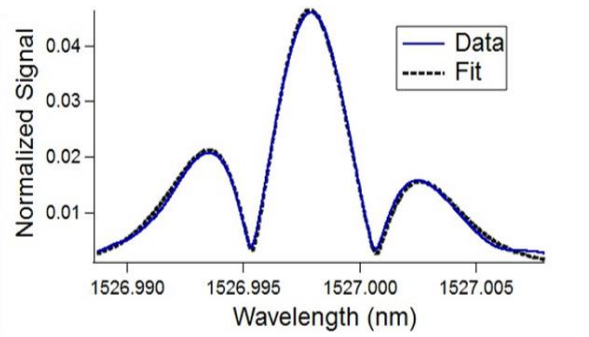

Figure 4: Fitted normalized signals (black) versus time averaged normalized signals (blue) for 1527nm NH_3 feature at 1mm downstream of nozzle exit.

The fitting procedure is repeated for each measurement location within the 81-point vertical scan at 1 mm downstream of the nozzle exit. The resulting areas for all three absorption features at each point within the scan are displayed in Figure 5 as a function of vertical position of the beam within the plume. The absorbance areas do not decrease to zero at the edges of the plume due to residual water vapor and ammonia within the vacuum chamber. To account for the residual signal, absorbance areas for all three absorption features are measured outside of the plume and are subtracted to isolate absorbance within the plume for temperature and species concentration calculations.

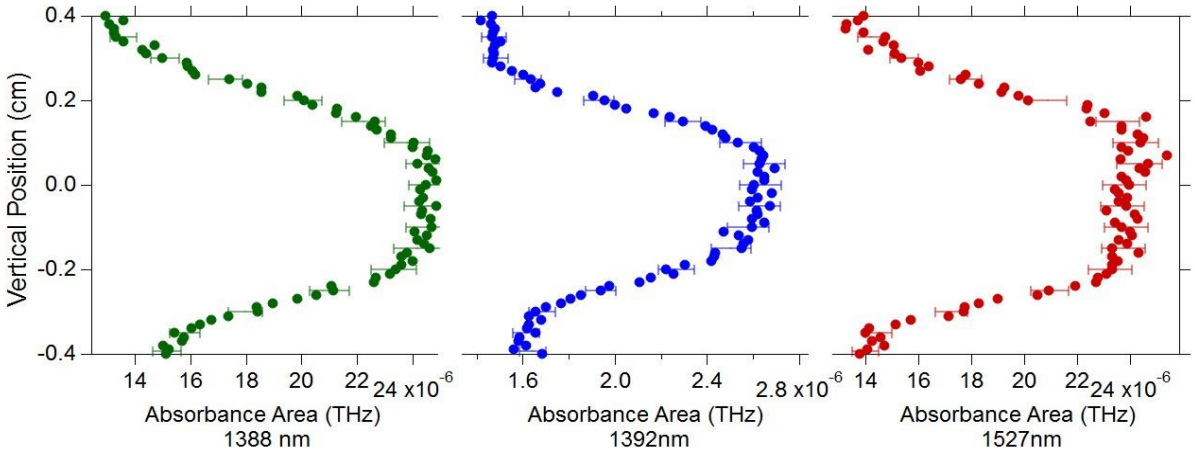

Figure 5: Absorbance areas as a function of vertical position in plume. a) Absorbance area of 1388nm H_2O feature. b) Absorbance area of 1392nm H_2O feature. c) Absorbance area of 1527nm NH_3 feature.

IV. Path Averaged Results

A. Temperature

Two-line thermometry, described by [12], is implemented to calculate the path averaged temperature within the plume. By taking the ratio of the calculated absorbance areas from the two H_2O absorption features, the measurement dependence on pressure, path length and species concentration is removed, as seen in Equation 3. Under these circumstances, the ratio of the absorbance areas, A_{1388} and A_{1392}, simplifies to the ratio of the linestrengths of the H_2O absorption features, $S_{1388}(T)$ and $S_{1392}(T)$, which are solely a function of temperature. Two-line thermometry is especially useful for plume measurements, as the plume width (L) and pressure distributions are not precisely known at each measurement location.

$$\frac{A_{1388}}{A_{1392}} = \frac{S_{1388}(T)X_{H2O}LP_{total}}{S_{1392}(T)X_{H2O}LP_{total}} = \frac{S_{1388}(T)}{S_{1392}(T)} \tag{3}$$

Using this approach, the path-averaged temperature at each point within the plume at 1mm downstream of the nozzle exit plane is calculated and shown in Figure 6. At the edges of the plume the absorbance signal from residual H_2O and NH_3 make up a larger percentage of the total measured signal, as the absorbance signal contributed from the plume decreases. This causes the uncertainty associated with the calculated background absorbance to be magnified at the edges of the plume as the background becomes a larger percentage of the signal.

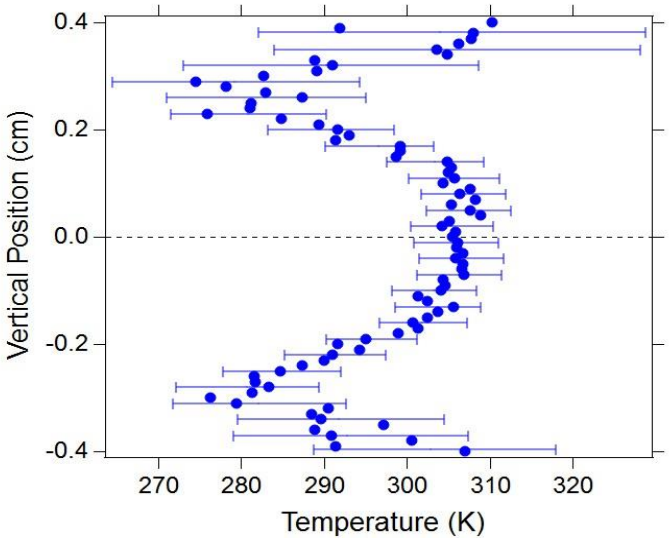

Figure 6: Path averaged temperature profile as a function of vertical position within the plume.

B. Species Concentration

Common methods for calculating species concentration in the plume are not effective for this application as the pathlength of the laser through the plume and the pressure distribution are unknown. Here we introduce a new method of species concentration measurement that is possible when one is measuring all of the species present in the flow. To begin, we calculate the ratio of the absorbance areas of one of the water absorbance features and the ammonia absorbance feature. Both absorbance areas were recorded at the same path length (L) and pressure (P_{total}), therefore the dependence on these parameters is removed (Equation 4).

In this system we assume there are no reactions taking place, therefore the only molecules within the system are the ammonia and water vapor. Under this situation, the sum of the mole fractions of ammonia and water are equal to one.

$$\frac{A_{1388}}{A_{1527}} = \frac{S_{1388}(T)X_{H2O}LP_{total}}{S_{1527}(T)X_{NH3}LP_{total}} = \frac{S_{1388}(T)X_{H2O}}{S_{1527}(T)X_{NH3}} \tag{4}$$

$$\sum_{i=1}^{N} X_i = 1 \rightarrow X_{NH3} + X_{H2O} = 1 \tag{5}$$

$$X_{NH3} = \frac{S_{1388}(T)A_{1527}}{A_{1388}S_{1527}(T) + A_{1527}S_{1388}(T)} \tag{6}$$

By combining Equations 4 and 5 and solving for the mole fraction of ammonia we arrive at Equation 6. Since the path averaged temperature has already been calculated, the right side of this equation is entirely known, enabling the calculation of the path-averaged mole fractions of the absorbing species at each location in the scan (see Figure 7). Since the vacuum chamber was evacuated prior to trials, we expect the mole fraction of NH_3 and H_2O to be approximately constant throughout the plume. The variation in mole fractions in Figure 7 is likely due to incomplete mixing of the NH_3 and H_2O prior to the nozzle, or non-linear temperature effects resulting from path averaged measurements over a range of temperatures. The large uncertainties on the edges of the plume is due to temperature uncertainty, which is reflected in linestrength uncertainty in Equation 6.

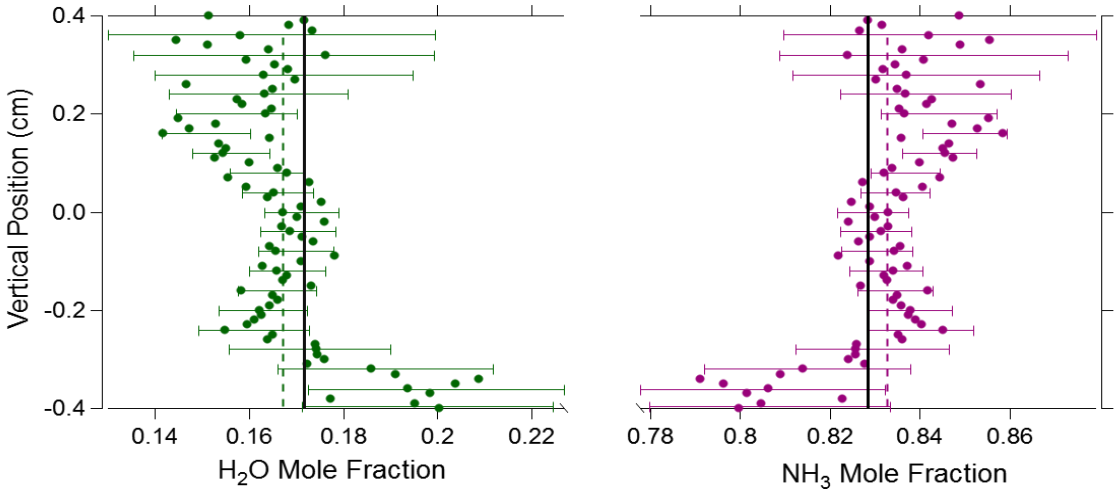

Figure 7: Water and ammonia mole fraction distributions in plume. Dashed lines represent the mean mole fraction of the data. Solid black lines represent the expected mole fraction based on the flow rates of H_2O and NH_3 into the chamber.

The dashed lines in Figure 7 represent the average mole fractions of H_2O and NH_3 from the data, 0.167±0.013 and 0.833±0.013 respectively. The solid black lines represent the expected mole fraction based on the flow rates of H_2O and NH_3 into the chamber, 0.172 and 0.828 respectively. The expected mole fractions fall well within one standard deviation of the calculated values. The agreement between expected values and measured values suggests that the proposed species concentration technique is valid for this application and that all significant constituents of the flow are accounted for.

Discrepancies in the measured mole fractions versus the expected mole fractions could be due to reactions taking place within the system, which we did not account for by assuming the only constituents in the flow were H_2O and NH_3, or from water vapor condensing out of the flow due to rapid temperature drops from the rapid expansion into the vacuum chamber. At the elevated temperatures, such as the temperature within the heaters (approximately 800K), NH_3 will partially to dissociate into N_2 and H_2 as in Equation 7. While the resident time the ammonia was kept at elevated temperatures was short, this reaction likely decreased the mole fraction of the NH_3 present in the system. This would also decrease the H_2O mole fraction since the total number of moles in the system is increased by this reaction.

$$2NH_3 \Leftrightarrow N_2 + 3H_2 \tag{7}$$

Although condensation is not observed within the system during testing, it is possible that the H_2O vapor is condensing in the flow, particularly at the edges of the plume where the temperatures are the lowest. Condensation would cause the vapor mole fraction of H_2O to decrease, while increasing the vapor mole fraction of NH_3. This is consistent with the calculated mole fractions being lower than the expected values in Figure 7.

V. Abel Transform Results

Given the radially symmetric nozzle geometry and the symmetry of the path averaged measurement results about the center axis of the nozzle exit, we assume that the plume is approximately axisymmetric. This allows the path averaged integrated absorbance measurements ($A_\lambda(y)$) from Figure 5 to be converted into integrated absorbance as a function of radius ($A'_\lambda(r)$), by the use of an inverse Abel transform (Equation 8). This method is described in depth in [13].

$$A'_\lambda(r) = -\frac{1}{\pi}\int_y^R \frac{dA_\lambda(y)}{dy}\frac{dy}{\sqrt{y^2 - r^2}} \tag{8}$$

We can reconstruct the radial temperature profile within the plume using two-line thermometry and the radial absorbance area distributions of the two H_2O features (Figure 8). From isentropic flow calculations for pure NH_3, we estimate that the temperature at the core of the plume at the exit of the nozzle should be approximately 350K. As our measurement is downstream of the exit plane, it is logical that the measured temperatures are lower than this predicted exit temperature. Computational fluid dynamics models would be required to determine the expected temperatures at the measurement location. The high temperature core and the low temperature edges of the plume are consistent with the expected nearfield under-expanded structure [14], [15]. As the optics are translated past to the plume boundary, we see the temperature return to near atmospheric temperature.

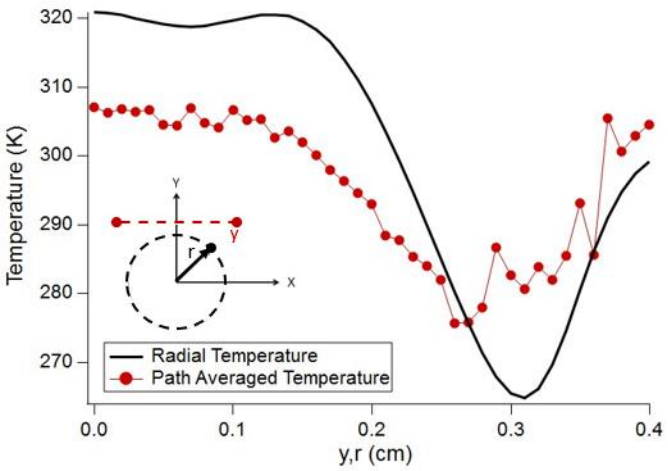

Figure 8: Radial temperature distribution from inverse Abel transform

VI. Conclusion

We resolve path-averaged and radial profiles of temperature within the plume of a small diameter (<5mm) converging-diverging nozzle expanding into a vacuum chamber at Edwards Air Force Base. A new method of calculating species mole fraction was proposed, for systems in which pressure and path length are uncertain, and for which all species are being measured. While the species mole fraction measurement technique includes some obvious sources of uncertainty, the uncertainties associated with estimating pressure and path length in a system such as this would be far greater. The calculated mole fractions compare well with expected values, indicating this mole fraction calculation technique is valid. Temperature results from path averaged and radially distributions agree with theoretical predictions, but a computational fluid dynamics model would be needed to fully validate this. The positive results from this study indicate that WMS could be applied to operational propulsion systems to gain temporally and spatially resolved measurements within the thruster plumes.

Acknowledgements

The University of Colorado authors were supported under contract ROS151366C from Jacobs Engineering. Helpful discussions with members of the Precision Laser Diagnostics Laboratory and AFRL In-Space Propulsion Branch are gratefully acknowledged.

References

[1] G. B. Rieker, J. B. Jeffries, and R. K. Hanson, "Calibration-free wavelength-modulation spectroscopy for measurements of gas temperature and concentration in harsh environments," *Appl. Opt.*, vol. 48, no. 29, p. 5546, Oct. 2009.

[2] J. A. Silver, "Frequency-modulation spectroscopy for trace species detection: theory and comparison among experimental methods," *Appl. Opt.*, vol. 31, no. 6, pp. 707–717, Feb. 1992.
[3] L. S. Rothman *et al.*, "The HITRAN2012 molecular spectroscopic database," *J. Quant. Spectrosc. Radiat. Transf.*, vol. 130, pp. 4–50, Nov. 2013.
[4] P. J. Schroeder *et al.*, "Dual Frequency Comb Spectroscopy of High Temperature Water Vapor: Absorption Model Development for Combustion Sensors," in *Light, Energy and the Environment (2016), paper FW2E.5*, 2016, p. FW2E.5.
[5] C. S. Goldenstein and R. K. Hanson, "Diode-laser measurements of linestrength and temperature-dependent lineshape parameters for H_2O transitions near 1.4 μm using Voigt, Rautian, Galatry, and speed-dependent Voigt profiles," *J. Quant. Spectrosc. Radiat. Transf.*, vol. 152, pp. 127–139, Feb. 2015.
[6] Michael Webber, "Diode Laser Measurements of NH_3 and CO_2 for Combustion and Bioreactor Applications," Stanford University, 2001.
[7] E. D. Hinkley and P. L. Kelley, "Detection of Air Pollutants with Tunable Diode Lasers," *Science*, vol. 171, no. 3972, pp. 635–639, Feb. 1971.
[8] L. Li, N. Arsad, G. Stewart, G. Thursby, B. Culshaw, and Y. Wang, "Absorption line profile recovery based on residual amplitude modulation and first harmonic integration methods in photoacoustic gas sensing," *Opt. Commun.*, vol. 284, no. 1, pp. 312–316, Jan. 2011.
[9] P. Kluczynski and O. Axner, "Theoretical description based on Fourier analysis of wavelength-modulation spectrometry in terms of analytical and background signals," *Appl. Opt.*, vol. 38, no. 27, pp. 5803–5815, Sep. 1999.
[10] K. Sun, X. Chao, R. Sur, C. S. Goldenstein, J. B. Jeffries, and R. K. Hanson, "Analysis of calibration-free wavelength-scanned wavelength modulation spectroscopy for practical gas sensing using tunable diode lasers," *Meas. Sci. Technol.*, vol. 24, no. 12, p. 125203, Dec. 2013.
[11] C. S. Goldenstein, C. L. Strand, I. A. Schultz, K. Sun, J. B. Jeffries, and R. K. Hanson, "Fitting of calibration-free scanned-wavelength-modulation spectroscopy spectra for determination of gas properties and absorption lineshapes," *Appl. Opt.*, vol. 53, no. 3, p. 356, Jan. 2014.
[12] R. K. Hanson and P. K. Falcone, "Temperature measurement technique for high-temperature gases using a tunable diode laser," *Appl. Opt.*, vol. 17, no. 16, p. 2477, Aug. 1978.
[13] C. Liu, L. Xu, F. Li, Z. Cao, S. A. Tsekenis, and H. McCann, "Resolution-doubled one-dimensional wavelength modulation spectroscopy tomography for flame flatness validation of a flat-flame burner," *Appl. Phys. B*, vol. 120, no. 3, pp. 407–416, Jun. 2015.
[14] J. McDaniel, C. Glass, D. Staack, and C. Miller, "Experimental and Computational Comparison of an Underexpanded Jet Flowfield," presented at the 40th AIAA Aerospace Sciences Meeting & Exhibit, Reno, NV, 2002.
[15] N. Suas-David, V. Kulkarni, A. Benidar, S. Kassi, and R. Georges, "Line shape in a free-jet hypersonic expansion investigated by cavity ring-down spectroscopy and computational fluid dynamics," *Chem. Phys. Lett.*, vol. 659, pp. 209–215, Aug. 2016.

Wavelength Modulation Spectroscopy for Temperature and Species Concentration in the Plume of a Supersonic Nozzle

A.S. Makowiecki [1], T.R.S. Hayden [1], M.R. Nakles [2], N. Pilgram [2], N.A. MacDonald [3], W.A. Hargus[3] and G.B. Rieker [1]

[1] University of Colorado Boulder
Boulder, Colorado
[2] ERC Incorporated
Edwards Air Force Base, CA
[3] Air Force Research Laboratory
Edwards Air Force Base, CA

July 10th, 2017

AIAA Propulsion and Energy Forum

Motivation

- **New chemical propellants are proposed for spacecraft systems**
- **Combustion chemistry is complex**
  - Diagnostics are required to validate models
- **Diagnostics are needed for lifetime analysis**
  - Determine the state-of-health of the system
- **Diagnostics include:**
  - Temperature
  - Species concentration

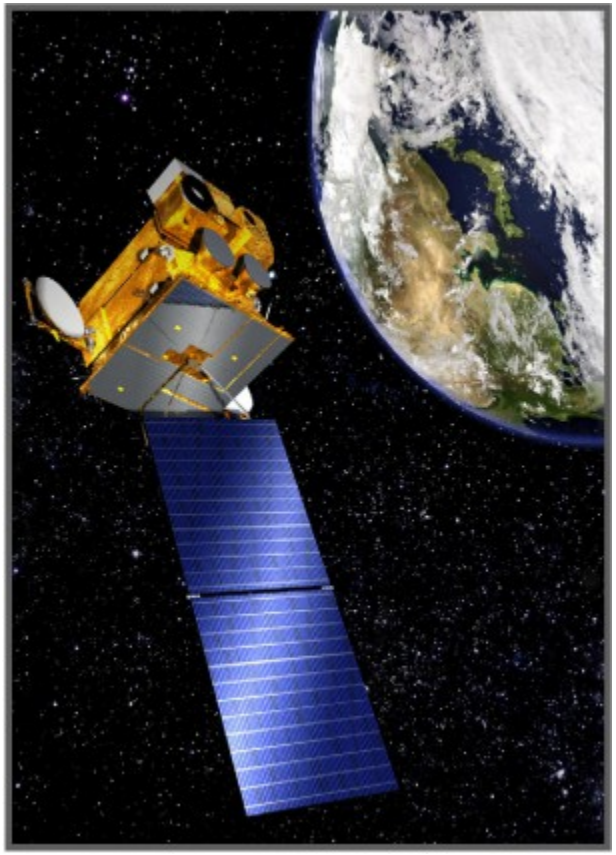

[1]

Approach

Goal:

Develop diagnostic tool for use in microthrusters for measurement of temperature and species concentration

Challenges:

- Ultra low pressure systems
- Small size
- Caustic chemicals
- Supersonic flow

Method:

Wavelength modulation spectroscopy validated in mock system

- Non-intrusive, in-situ measurements:
  - Temperature
  - Species concentration
- Quantitative and calibration free

Presentation Outline

1) **Motivation and Approach**
2) **Introduction to Absorption Spectroscopy**
   - Direct Absorption
   - Wavelength Modulation Spectroscopy
3) **Testing**
   - Optical system
   - Experimental setup
   - Scanning path
4) **Results**
   - Data processing
   - Absorbance area
   - Temperature measurements
     - **Path averaged**
     - **Abel inversion**
   - Species Concentration
5) **Conclusions and Acknowledgements**

Presentation Outline

1) **Motivation and Approach**
2) **Introduction to Absorption Spectroscopy**
   - Direct Absorption
   - Wavelength Modulation Spectroscopy
3) **Testing**
   - Optical system
   - Experimental setup
   - Scanning path
4) **Results**
   - Data processing
   - Absorbance area
   - Temperature measurements
     - **Path averaged**
     - **Abel inversion**
   - Species Concentration
5) **Conclusions and Acknowledgements**

Absorption Spectroscopy

- **Molecules absorb light at discrete wavelengths resonant with molecular transitions**

- **The amount of light absorbed is related to:**

$$\alpha(\lambda) = S(T)PXL\Phi$$

  - Line-strength: $S(T)$
  - Pressure: P
  - Mole fraction: X
  - Pathlength: L
  - Line-shape function: ϕ

- **Parameters $S(T)$ and ϕ are unique to each transition**
  - HITRAN2012 [3]
  - Experimental validations [4,5]

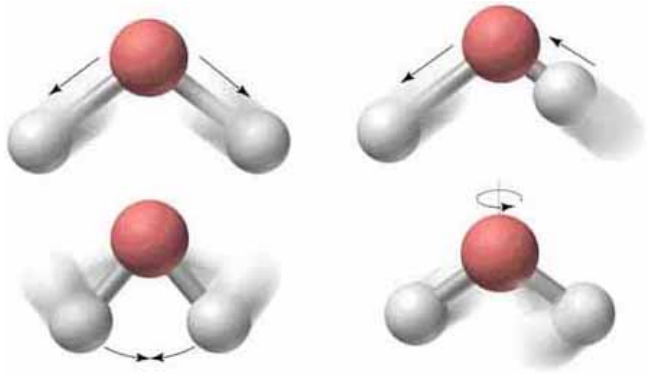

[2]

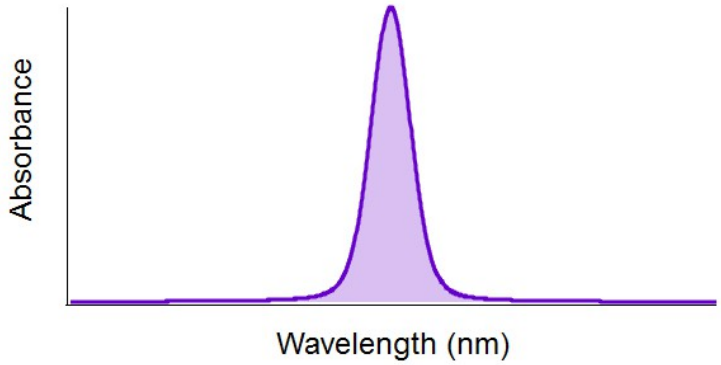

Tunable Diode Laser Absorption Spectroscopy (TDLAS)

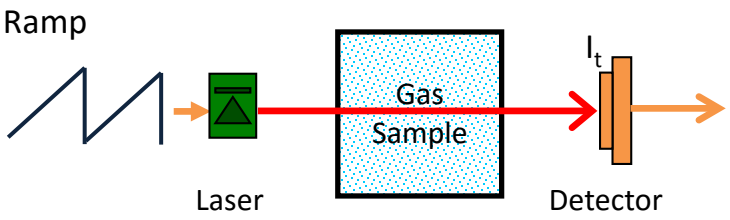

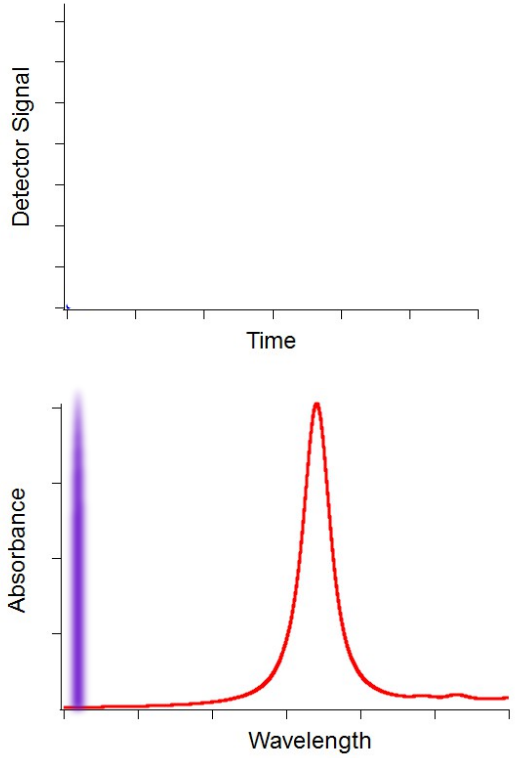

Tunable Diode Laser Absorption Spectroscopy (TDLAS)

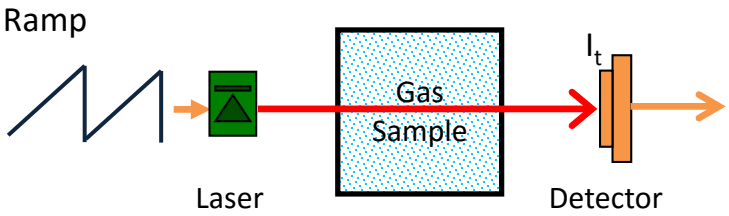

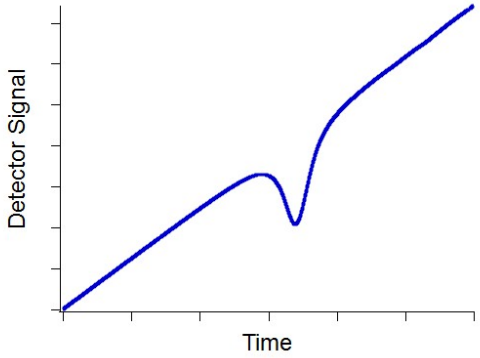

$$\alpha(\lambda) = S(T)PXL\Phi = -ln(\frac{I}{I_o})$$

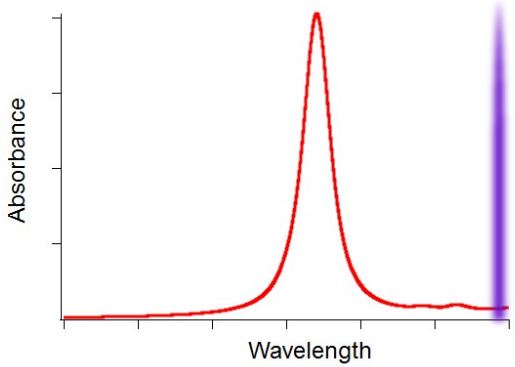

Wavelength Modulation Spectroscopy

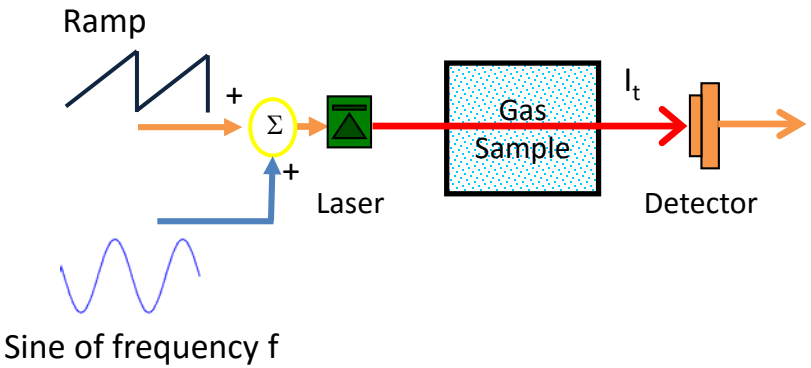

Wavelength Modulation Spectroscopy

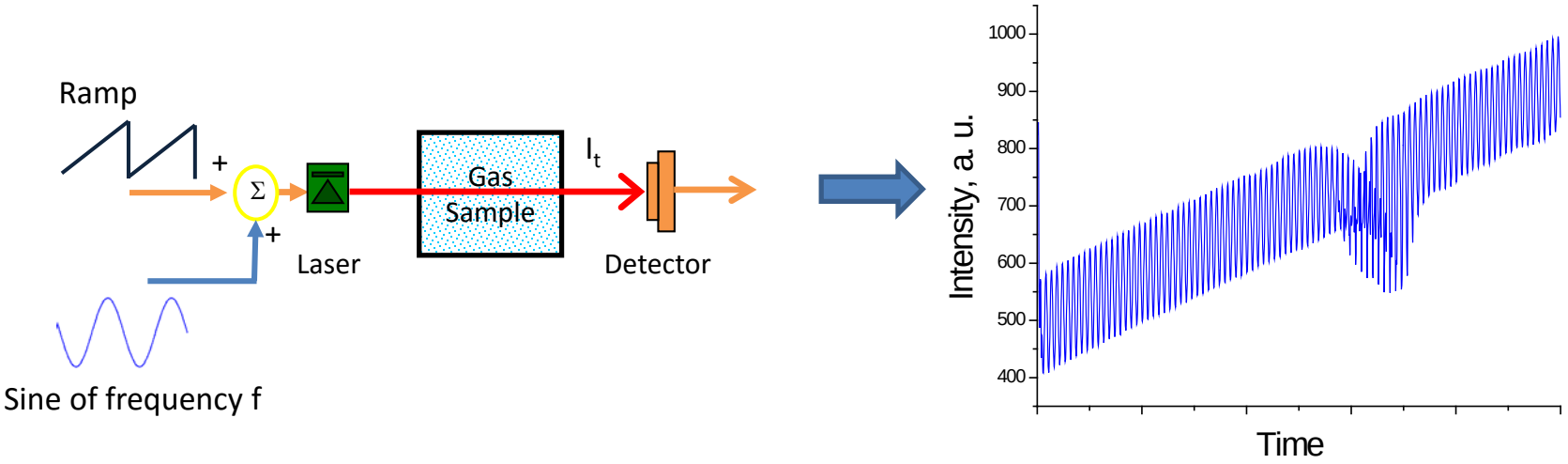

Wavelength Modulation Spectroscopy

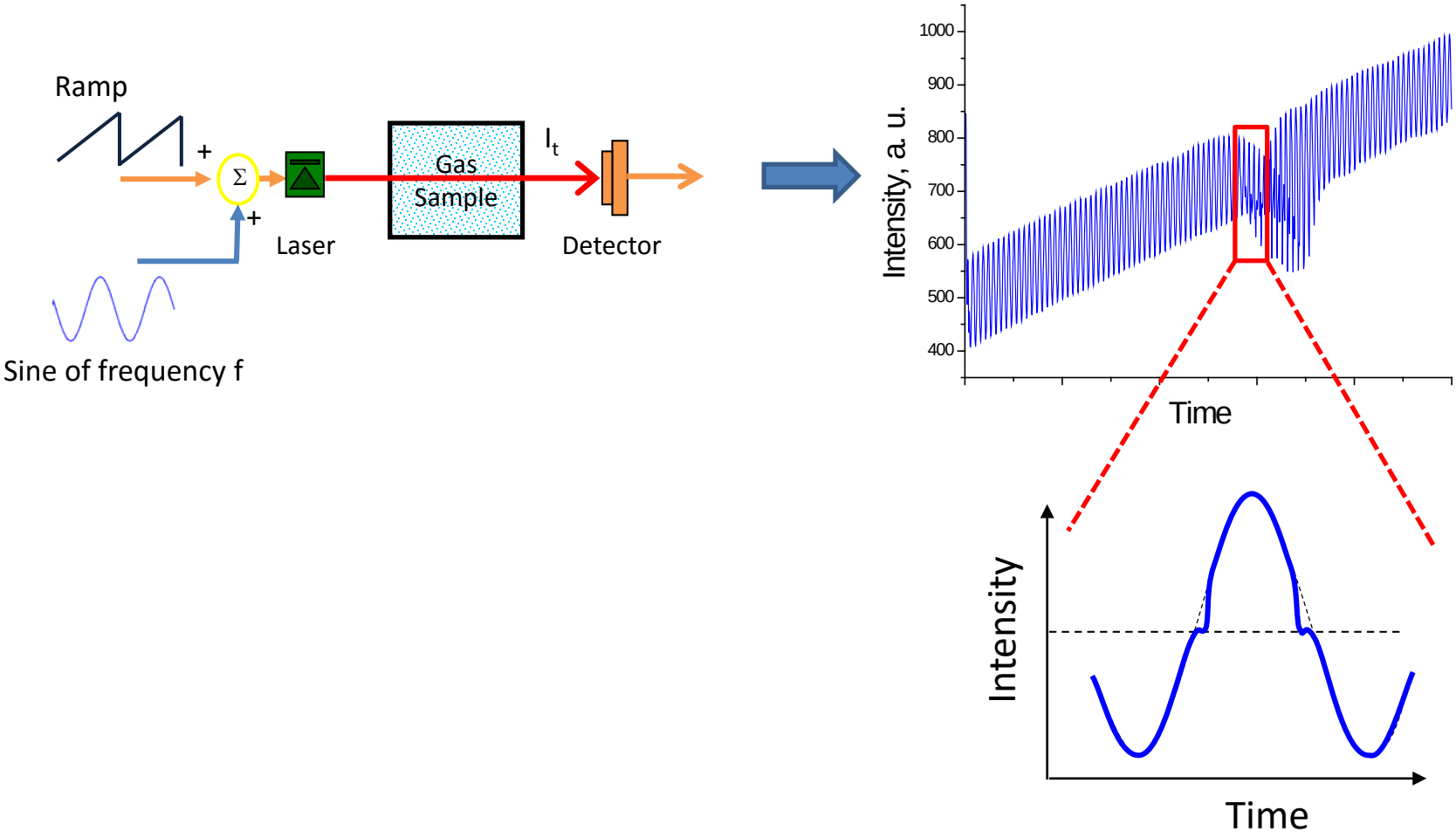

Wavelength Modulation Spectroscopy

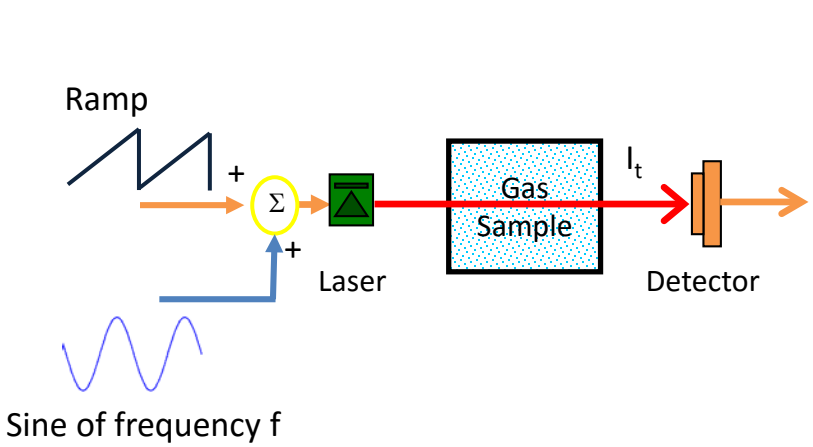

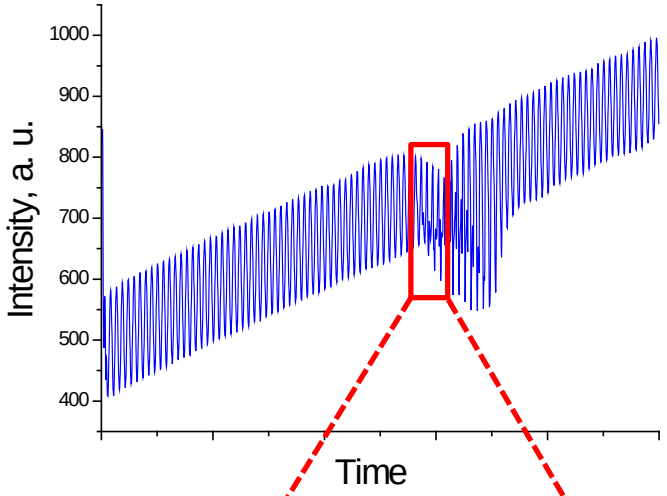

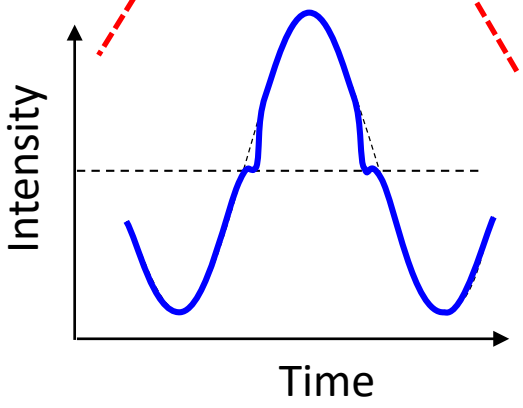

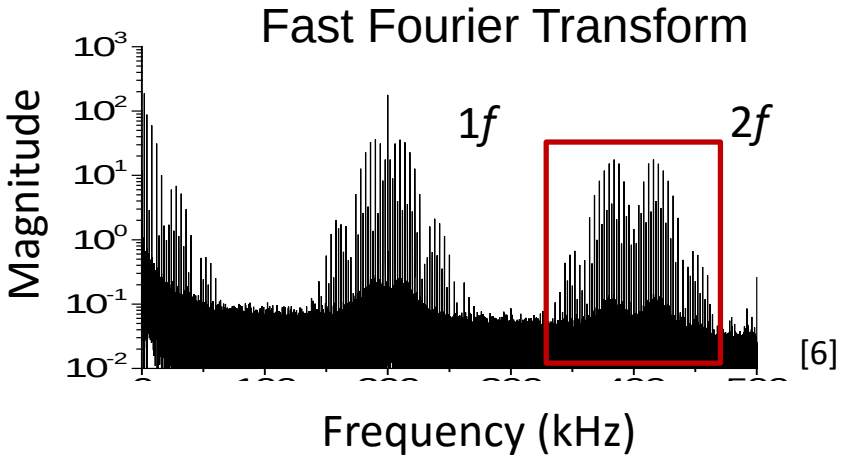

Wavelength Modulation Spectroscopy

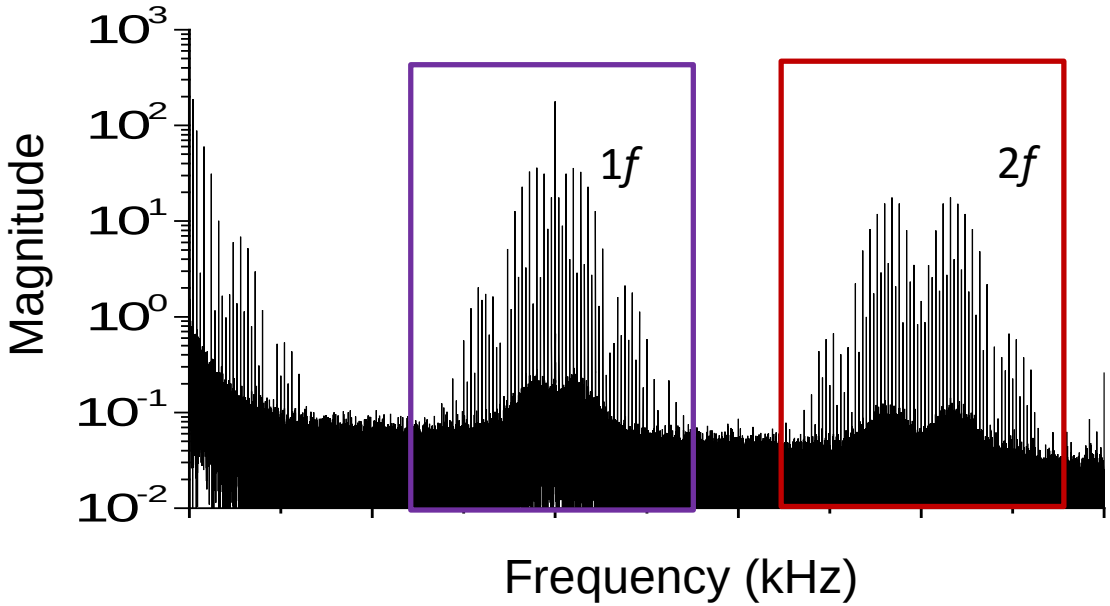

[6]

Wavelength Modulation Spectroscopy

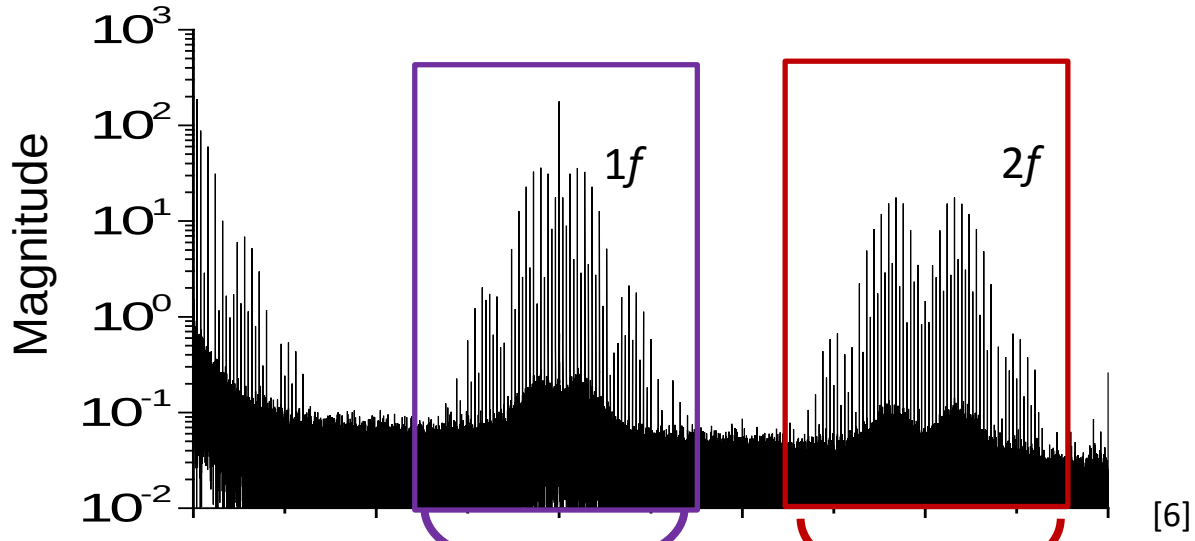

[6]

Apply lockin amplifier

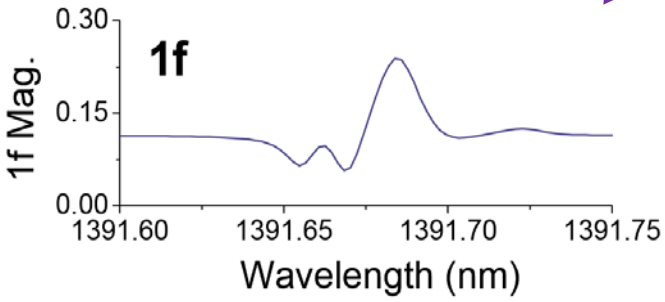

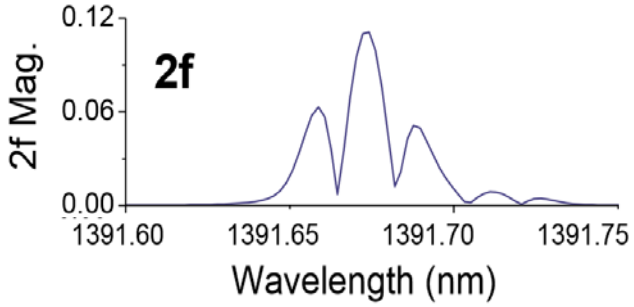

Wavelength Modulation Spectroscopy

- **Normalizing the 2f signal by the 1f signal removes dependence on laser intensity**
- **Important in harsh environments**
  - Window fouling
  - Vibrating optics

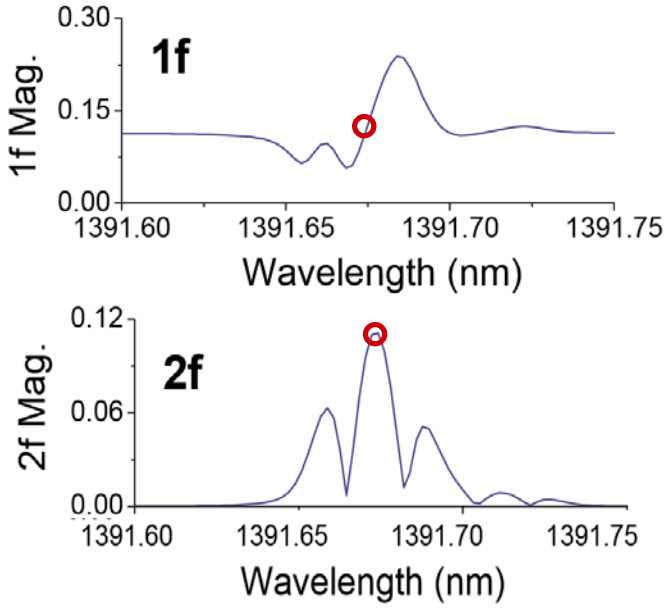

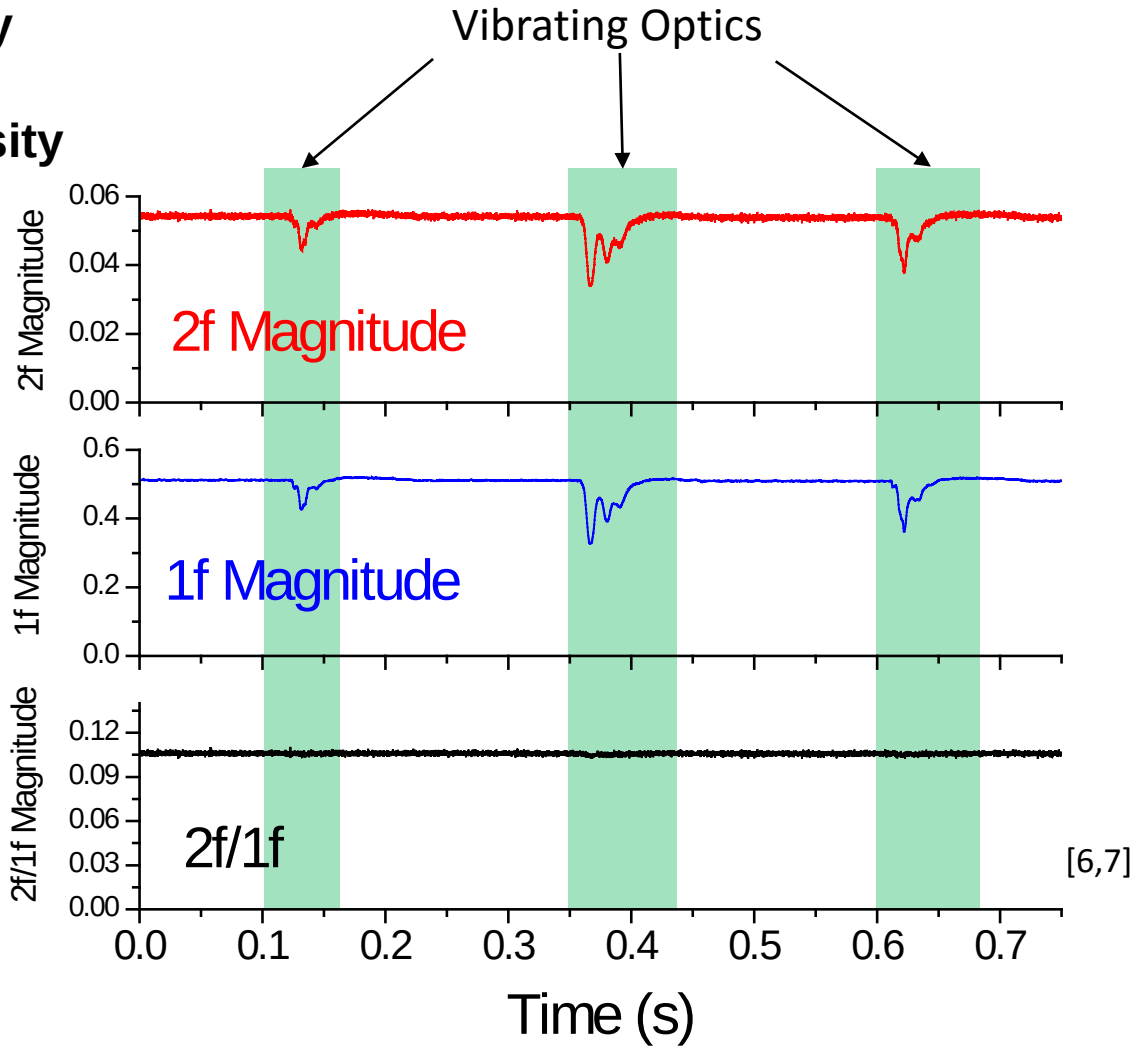

[6,7]

Data Processing

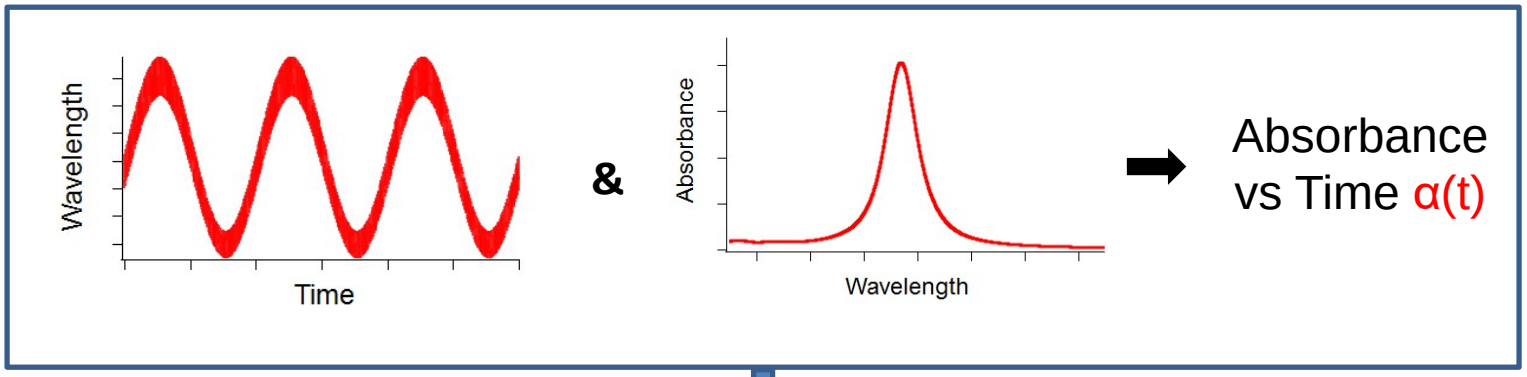

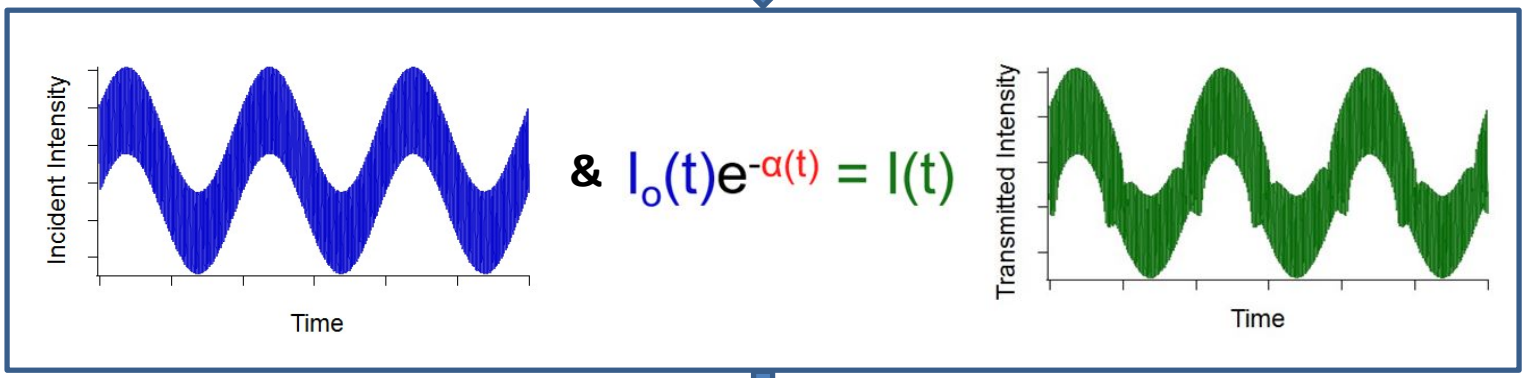

Run resulting I(t) through lockin to generate a simulated signal. Compare

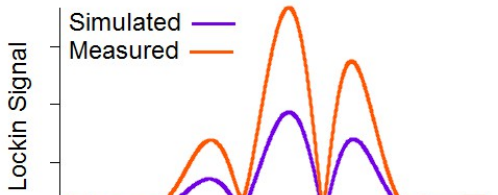

[8,9]

Temperature Measurement

Temperature can be calculated from the ratio of the absorbance areas of two well chosen absorption features

$$\text{Absorbance area ratio} = \frac{S1(T)PXL}{S2(T)PXL}$$

[10]

Temperature Measurement

Temperature can be calculated from the ratio of the absorbance areas of two well chosen absorption features

$$\text{Absorbance area ratio} = \frac{S1(T)\cancel{PXL}}{S2(T)\cancel{PXL}} = \frac{S1(T)}{S2(T)}$$

[10]

Temperature Measurement

Temperature can be calculated from the ratio of the absorbance areas of two well chosen absorption features

$$\text{Absorbance area ratio} = \frac{S1(T)\cancel{PXL}}{S2(T)\cancel{PXL}} = \frac{S1(T)}{S2(T)}$$

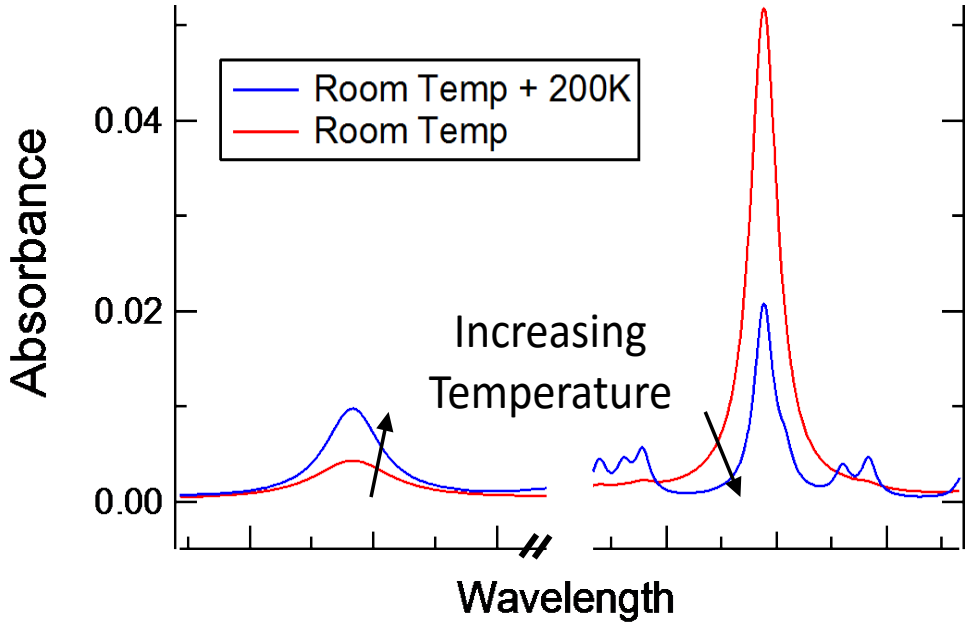

[10]

Temperature Measurement

Temperature can be calculated from the ratio of the absorbance areas of two well chosen absorption features

$$\text{Absorbance area ratio} = \frac{S1(T)\cancel{PXL}}{S2(T)\cancel{PXL}} = \frac{S1(T)}{S2(T)}$$

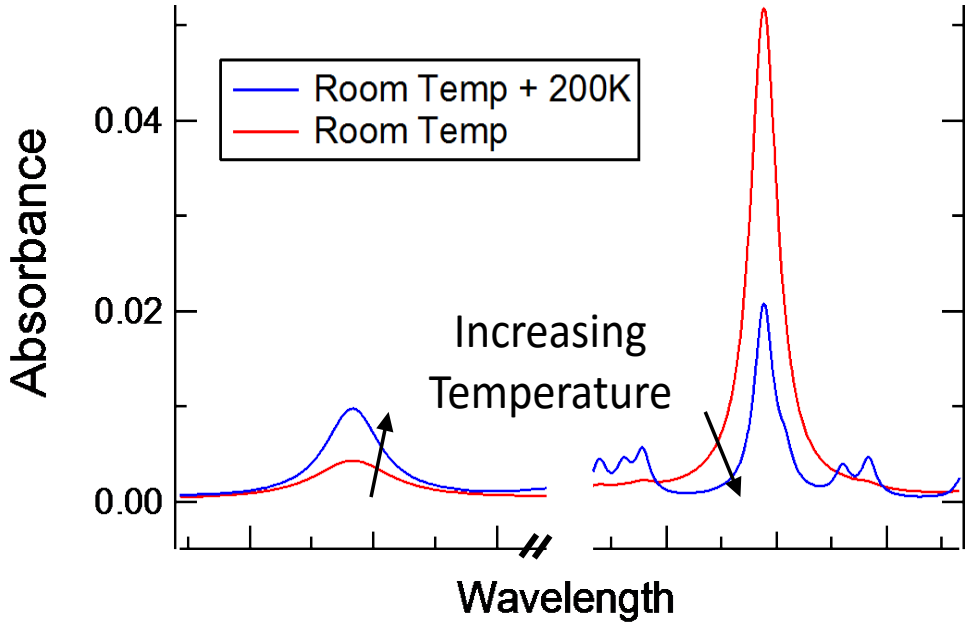

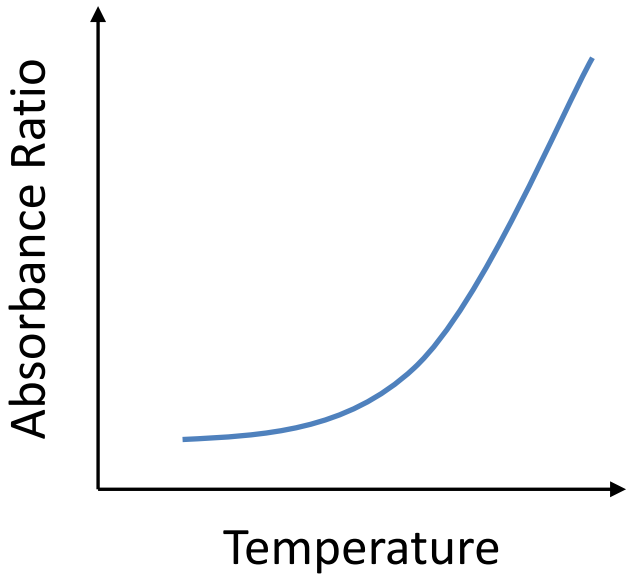

[10]

Temperature Measurement

Temperature can be calculated from the ratio of the absorbance areas of two well chosen absorption features

$$\text{Absorbance area ratio} = \frac{S1(T)\cancel{PXL}}{S2(T)\cancel{PXL}} = \frac{S1(T)}{S2(T)}$$

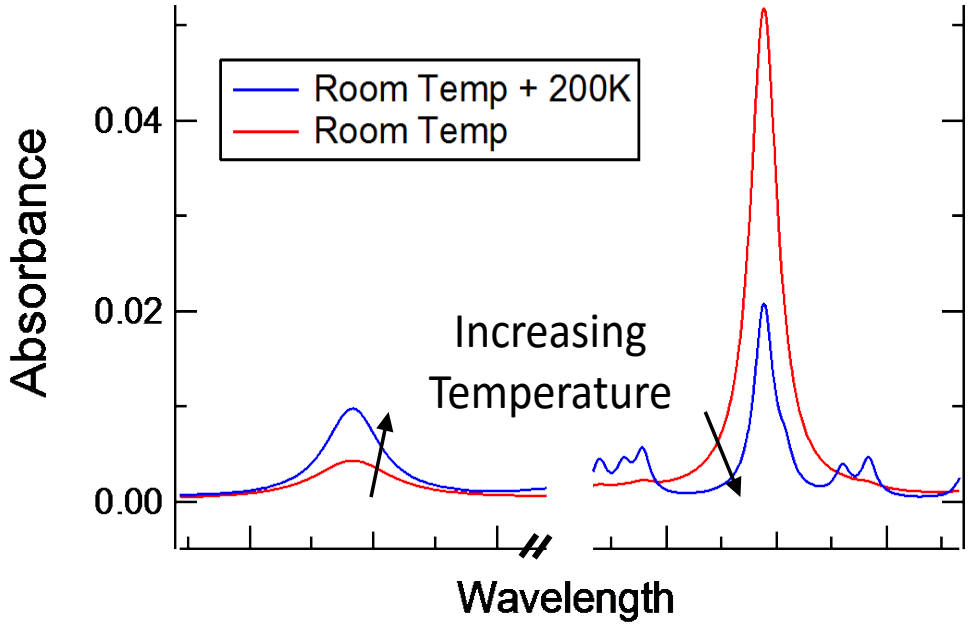

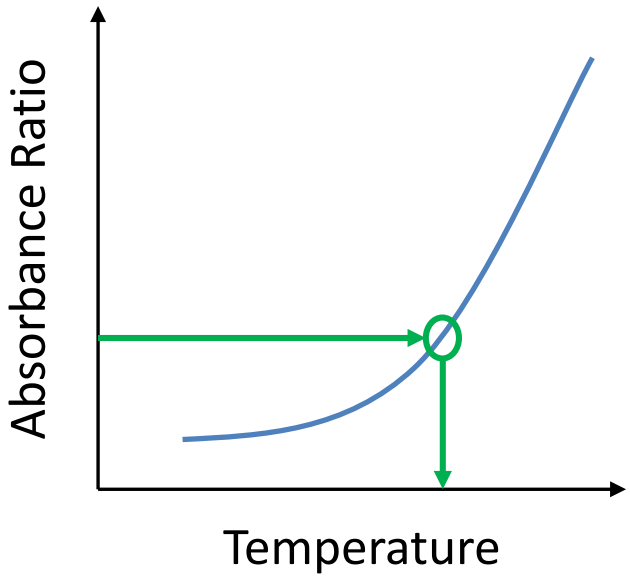

[10]

Presentation Outline

1) **Motivation and Approach**
2) **Introduction to Absorption Spectroscopy**
   - Direct Absorption
   - Wavelength Modulation Spectroscopy
3) **Testing**
   - Optical system
   - Experimental setup
   - Scanning path
4) **Results**
   - Data processing
   - Absorbance area
   - Temperature measurements
     - **Path averaged**
     - **Abel inversion**
   - Species Concentration
5) **Conclusions and Acknowledgements**

System Design

- **Testing performed at the AFRL at Edwards Air Force Base**
  - Vacuum chamber 4 within the Spacecraft Propulsion Laboratory
- **System developed by the AFRL**
  - Exhaust products: NH_3 and H_2O
  - Expansion ratio: 5.19
  - Exit Mach number: 3.1
- **LabView controlled translation stage mounted downstream**

Spectroscopy System

- **Spectroscopy system developed at CU Boulder**
  - Verification of NH_3 and H_2O line parameters in furnace
  - Characterized laser operating conditions
  - Developed simulation procedures
- **Measurements**
  - Temperature distributions
  - H_2O concentration
  - NH_3 concentration
- **Three Near-IR lasers**
  - 1388nm (H_2O)
  - 1392nm (H_2O)
  - 1527nm (NH_3)

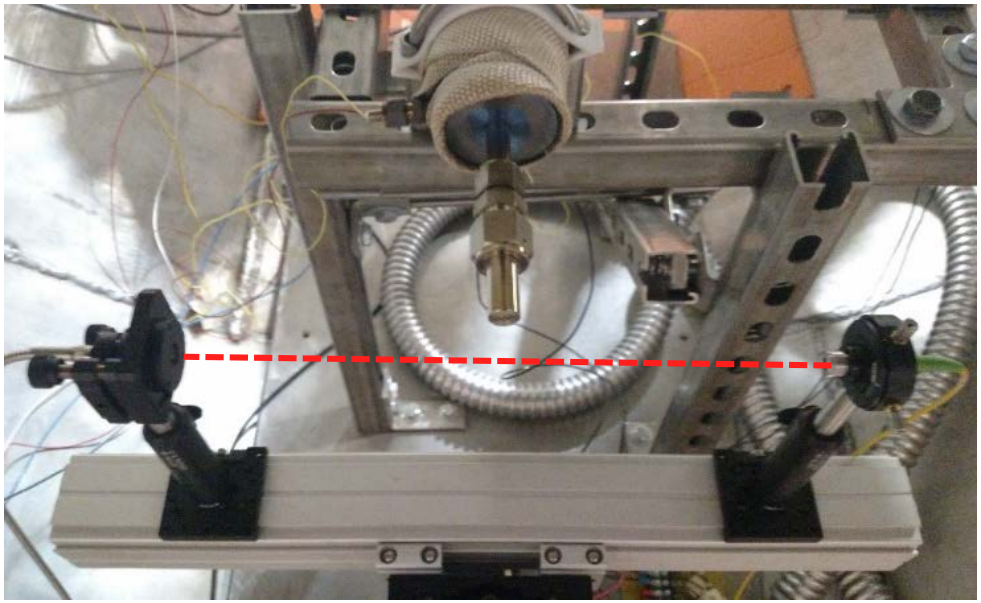

Experimental Setup

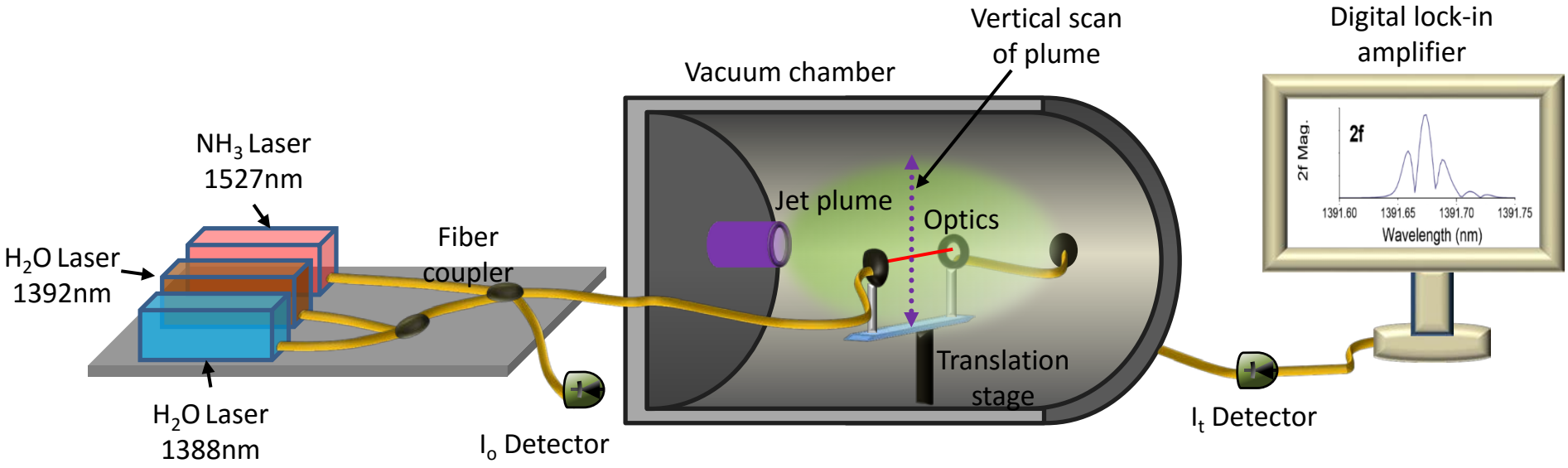

Scanning Path

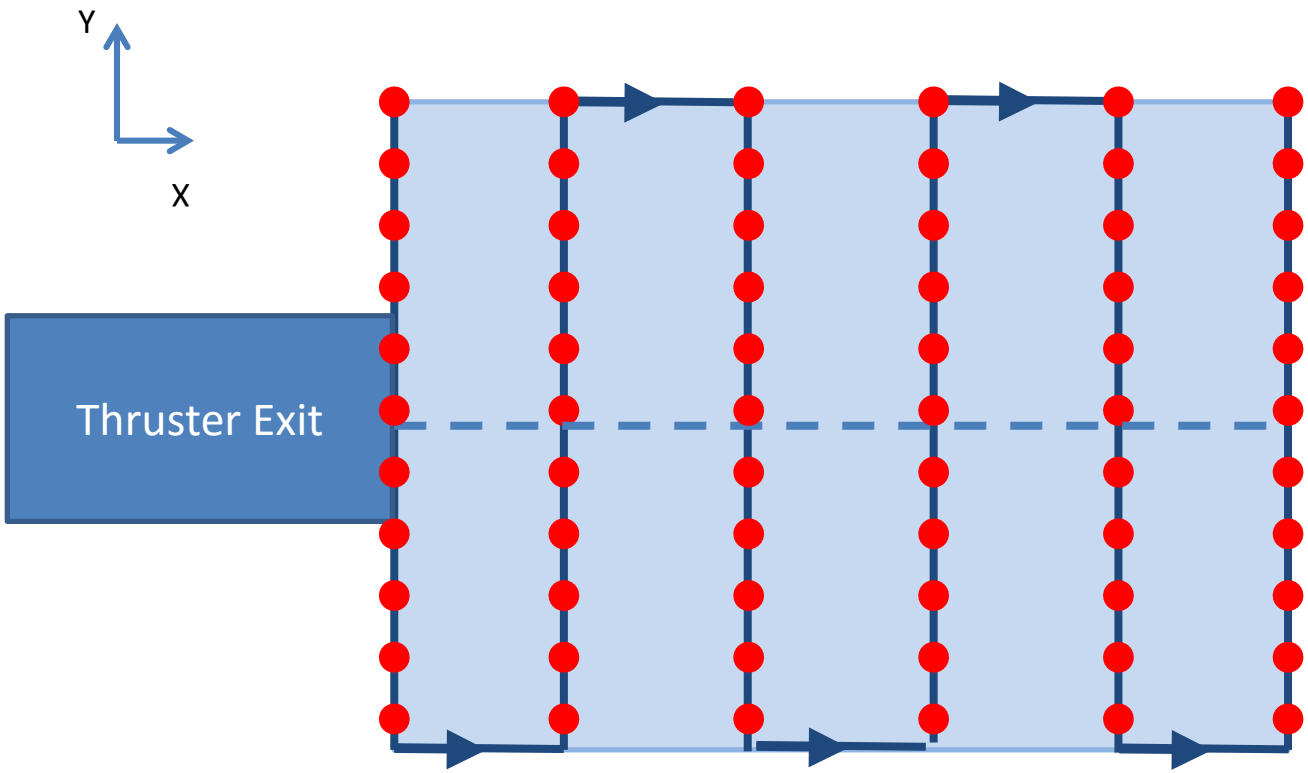

x = 1 mm (from exit plane of nozzle), 81 point vertical scan, Δy = 0.1 mm

Scanning Path

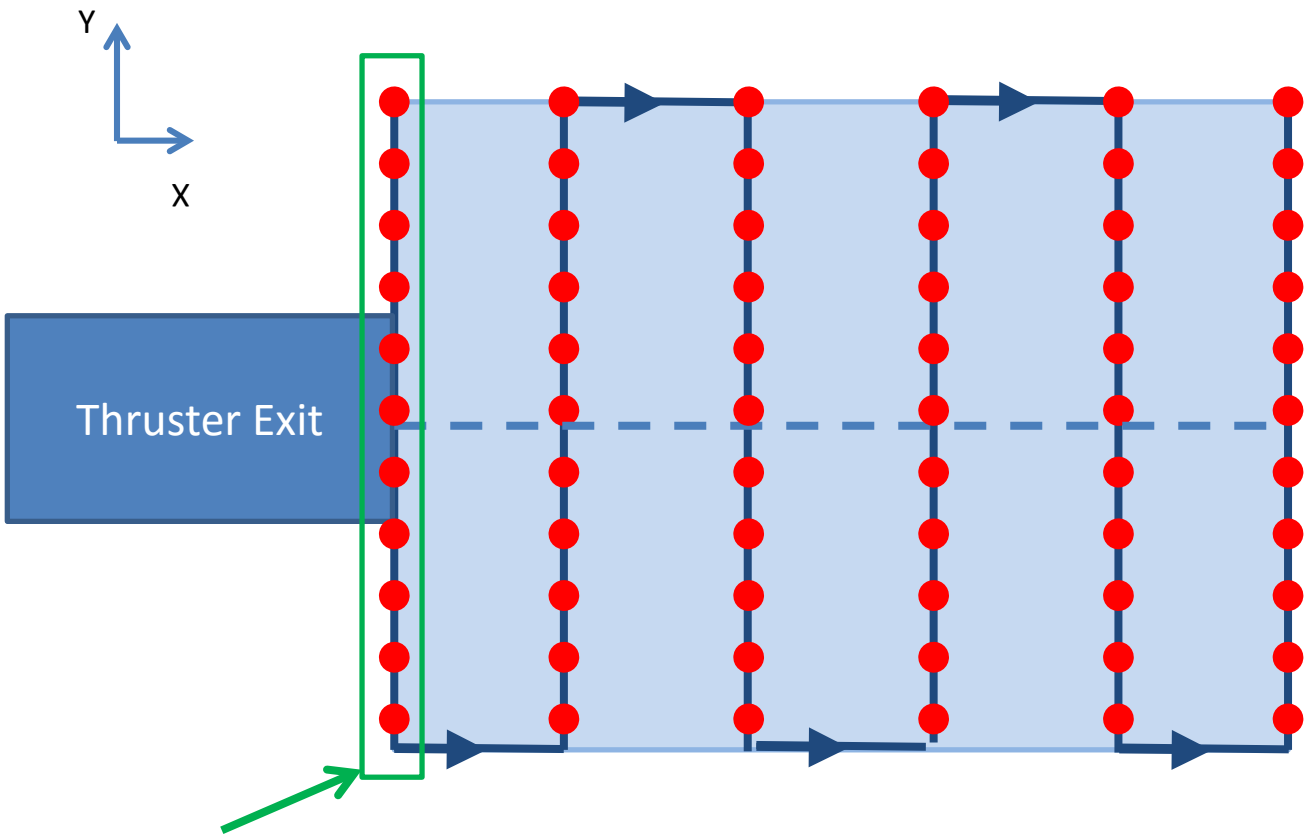

x = 1 mm (from exit plane of nozzle), 81 point vertical scan, Δy = 0.1 mm

Presentation Outline

1) **Motivation and Approach**
2) **Introduction to Absorption Spectroscopy**
   - Direct Absorption
   - Wavelength Modulation Spectroscopy
3) **Testing**
   - Optical system
   - Experimental setup
   - Scanning path
4) **Results**
   - Data processing
   - Absorbance area
   - Temperature measurements
     - **Path averaged**
     - **Abel inversion**
   - Species Concentration
5) **Conclusions and Acknowledgements**

Data Processing

Water absorption features

Typical fit for 1388nm signal (H_2O)

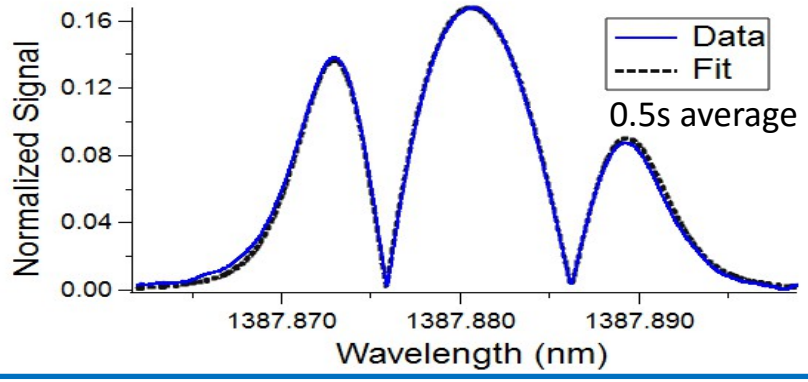

Typical fit for 1392nm signal (H_2O)

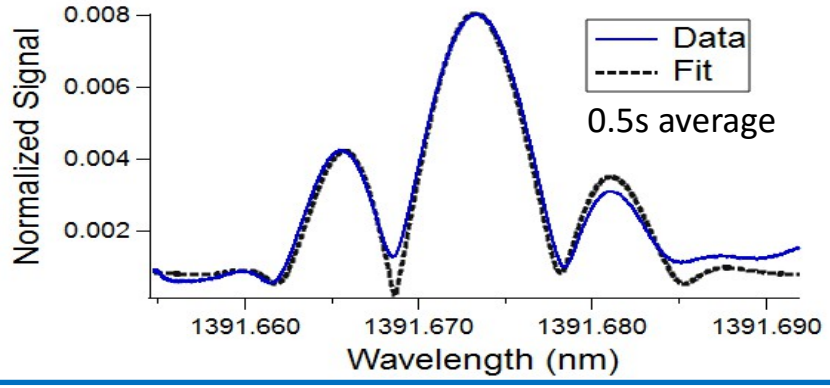

NH_3 absorption feature

Typical fit for 1527nm signal (NH_3)

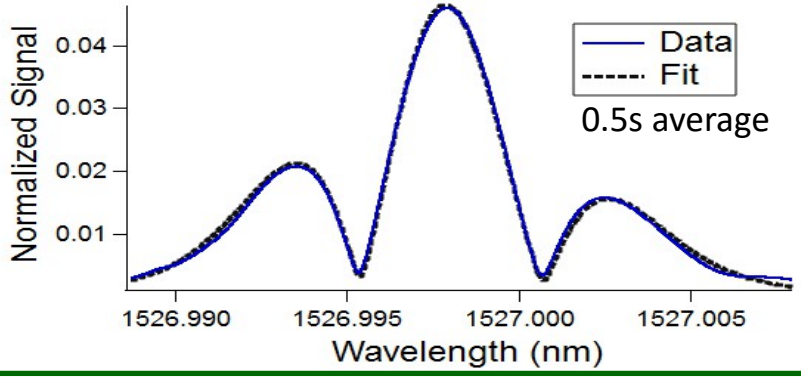

Good agreement between the simulated signal and the fit indicate correct absorbance parameters

[8,9]

Absorbance Area

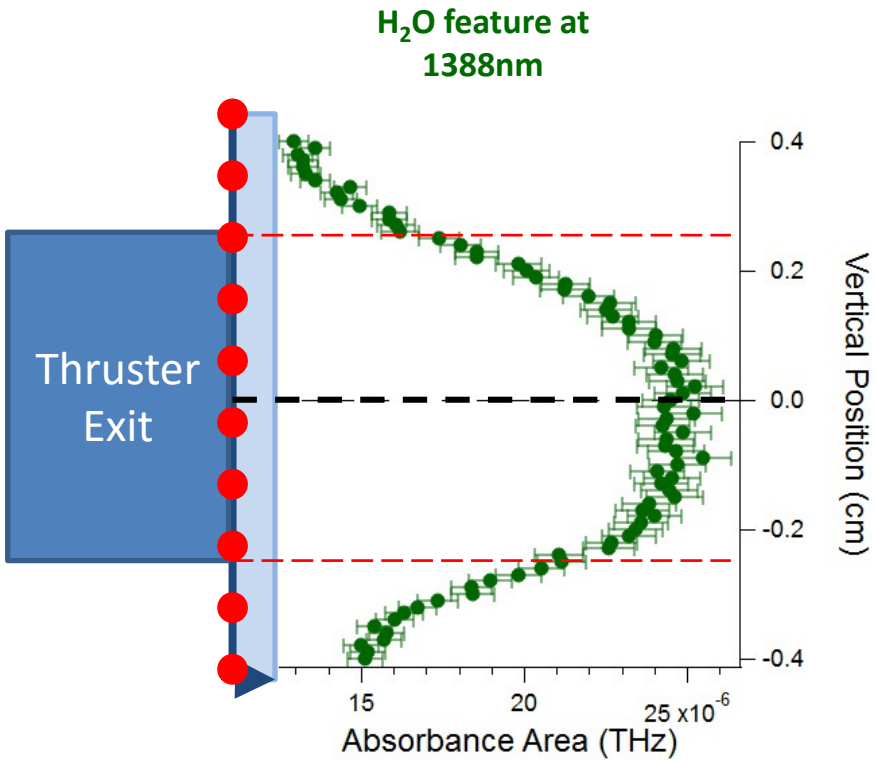

Data recorded at 1mm from exit plane of thruster

Absorbance Area

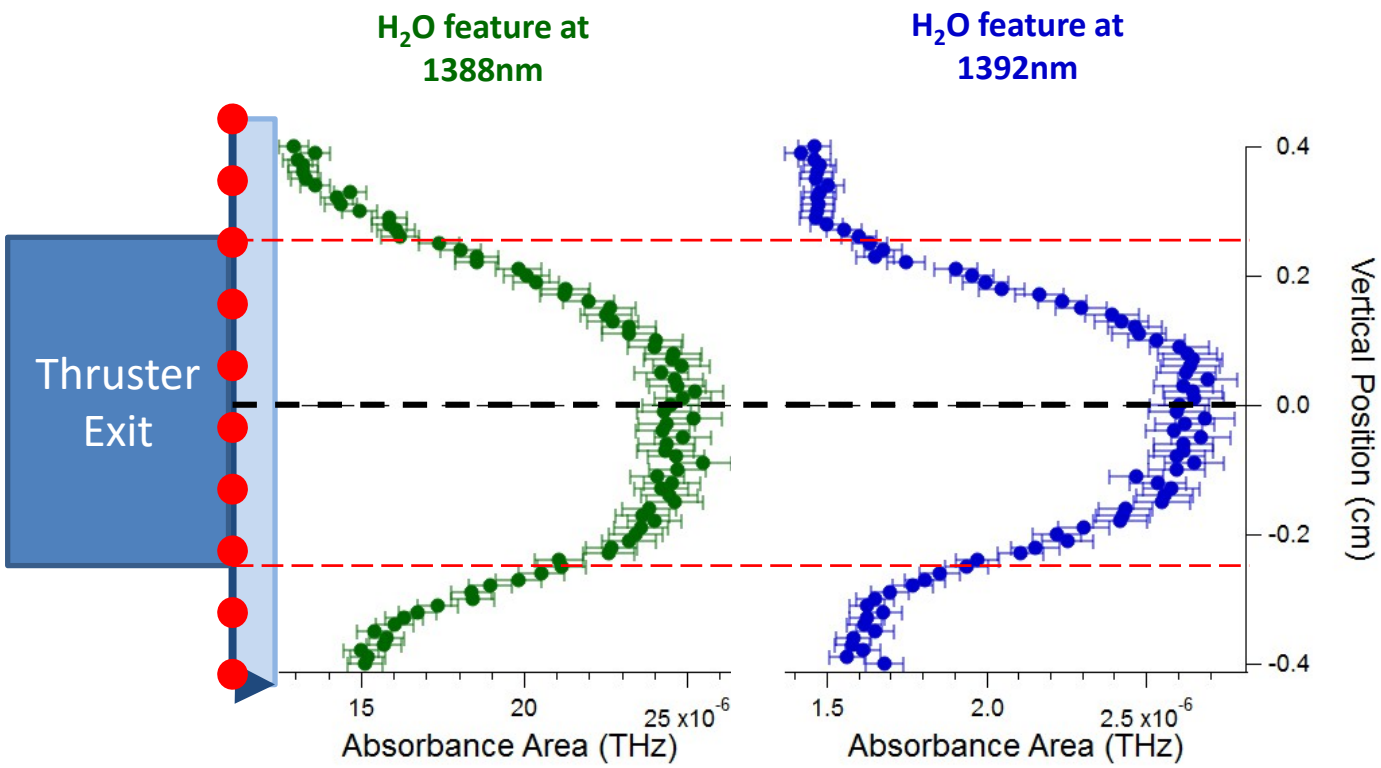

Data recorded at 1mm from exit plane of thruster

Absorbance Area

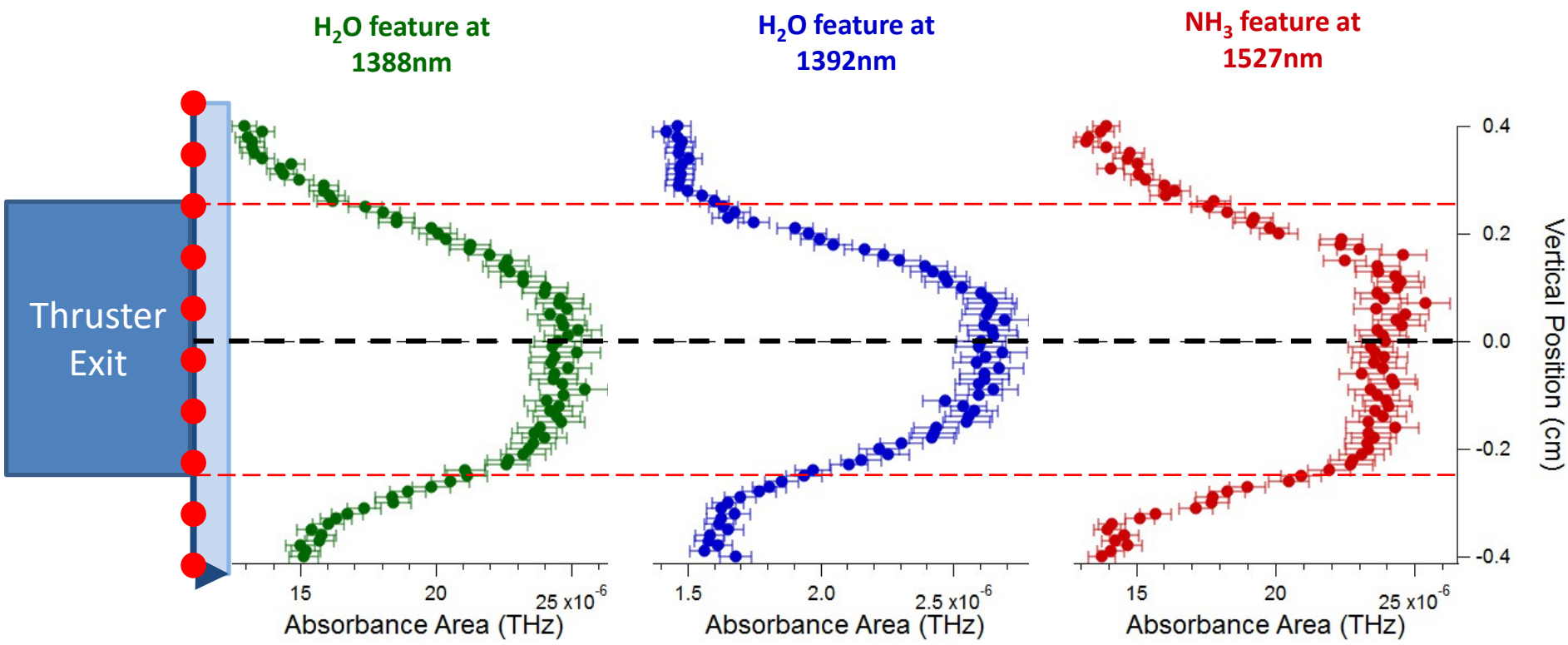

Data recorded at 1mm from exit plane of thruster

Temperature Measurement

Temperature can be calculated from the ratio of the areas for 1388nm and 1392nm absorption features

$$\text{Absorbance area ratio} = \frac{S(1388)\cancel{PXL}}{S(1392)\cancel{PXL}} = \frac{S(1388)}{S(1392)}$$

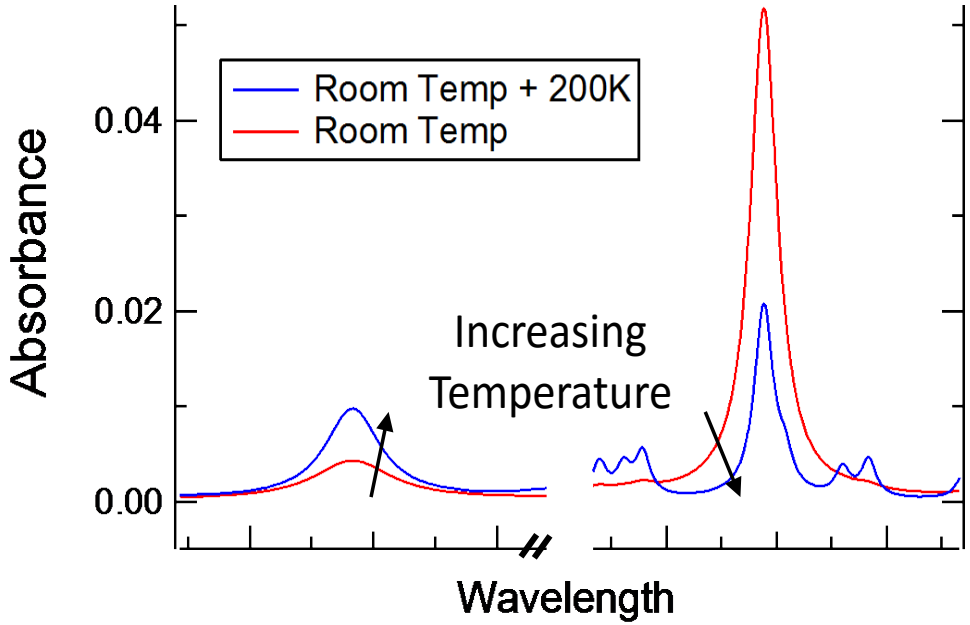

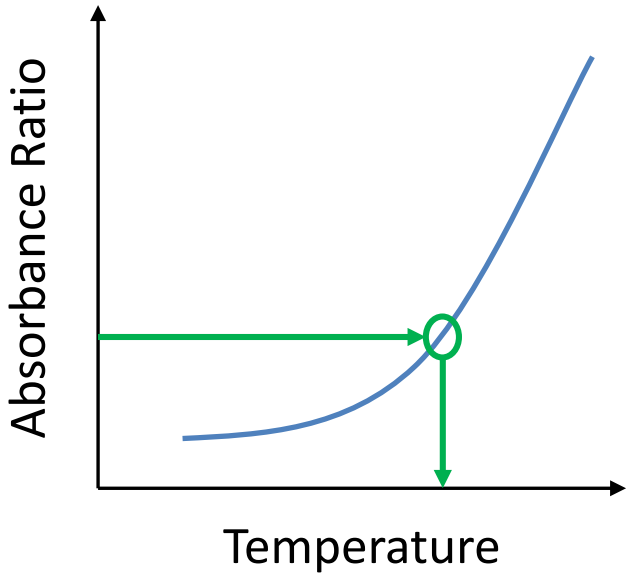

[10]

Temperature Measurement

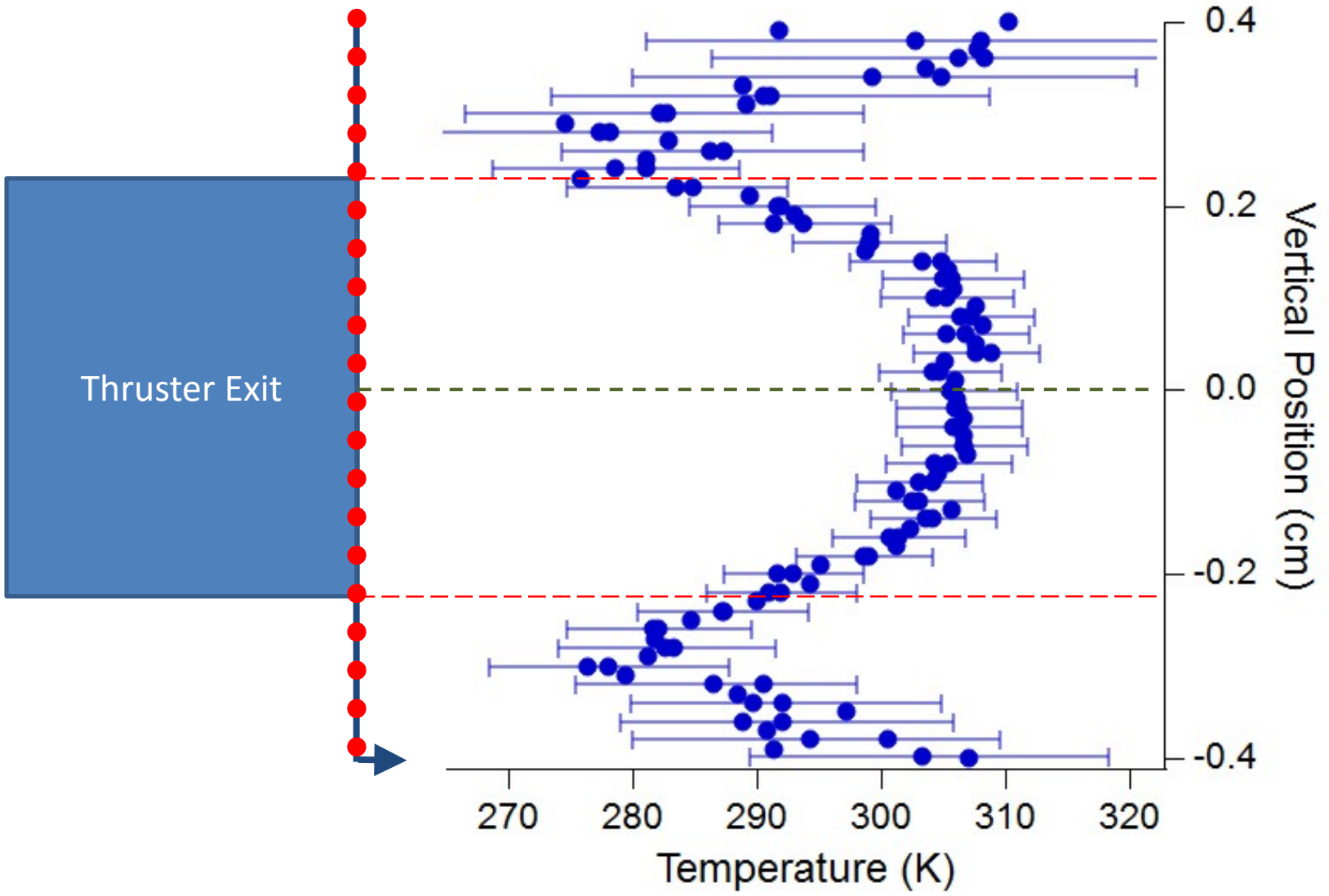

Inverse Abel Transform

- **Apply inverse Abel transform to path averaged measurements**
  - Assuming axisymmetric flow
  - Calculate radial distributions
  - Use “Fourier Method” to approximate F(y) as a cosine expansion

$$f(r) = -\frac{1}{\pi}\int_{y}^{R}\frac{dF(y)}{dy}\frac{dy}{\sqrt{y^2 - r^2}}$$

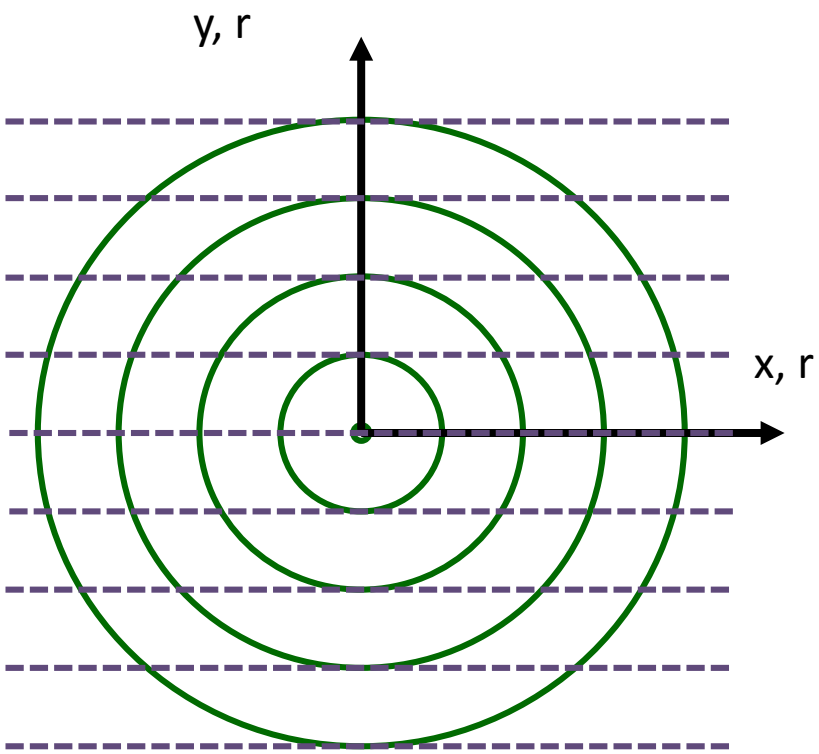

[11,12]

Inverse Abel Transform

Absorbance Area of 1388 Feature

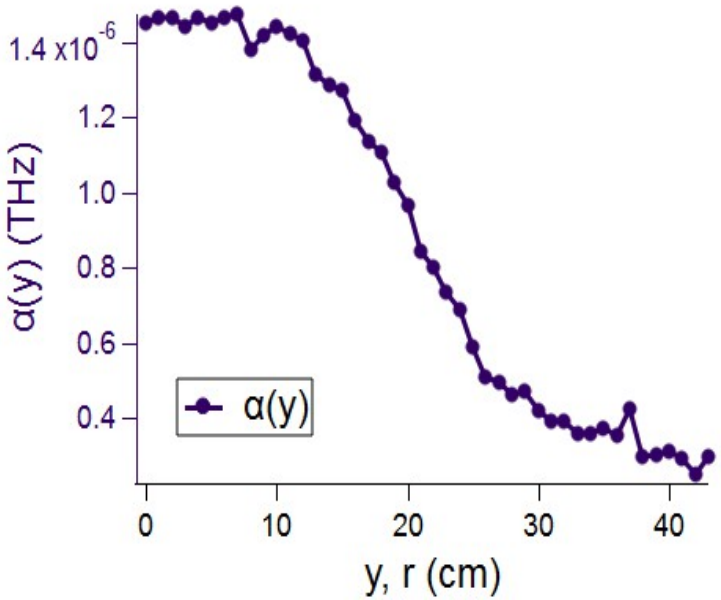

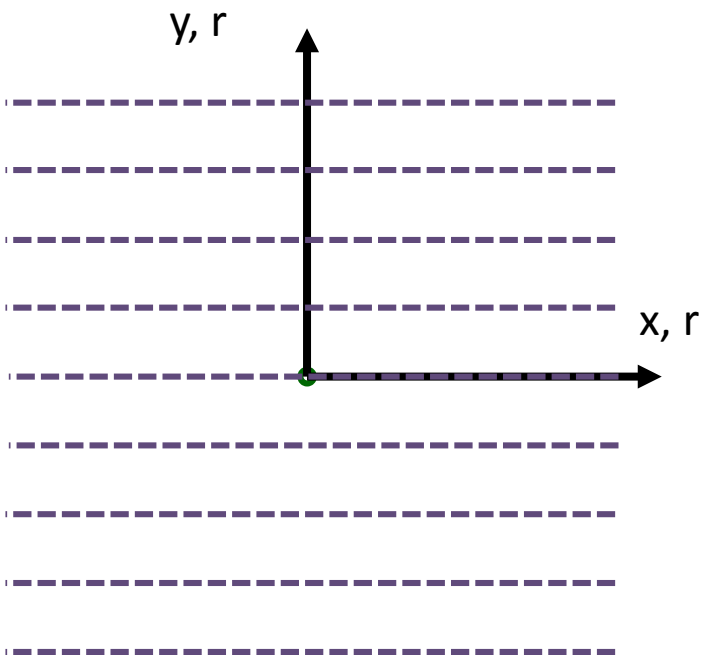

[11,12]

Inverse Abel Transform

Absorbance Area of 1388 Feature

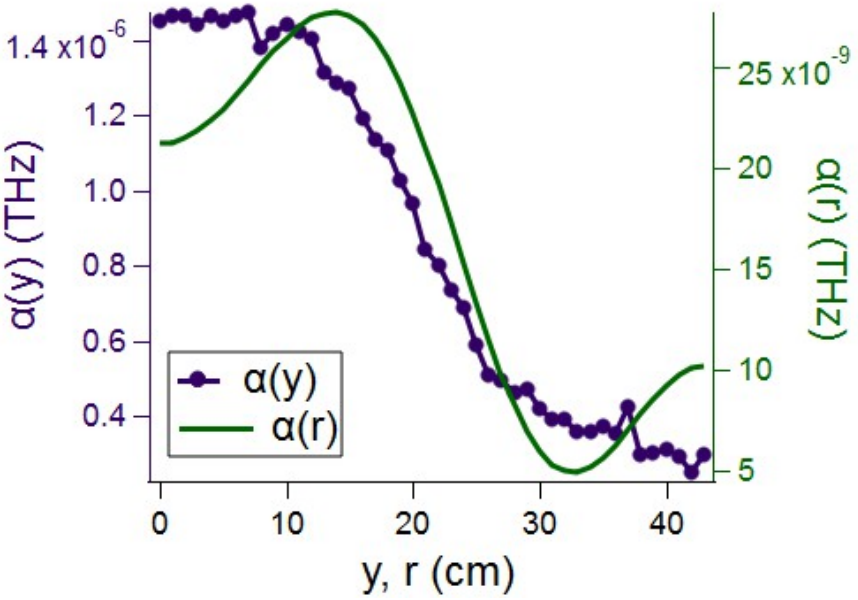

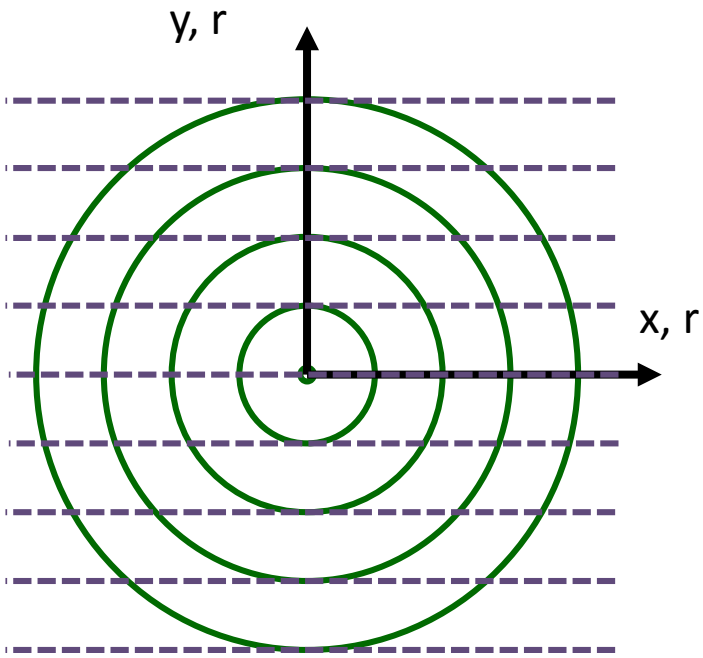

[11,12]

Inverse Abel Transform

Absorbance Area of 1388 Feature

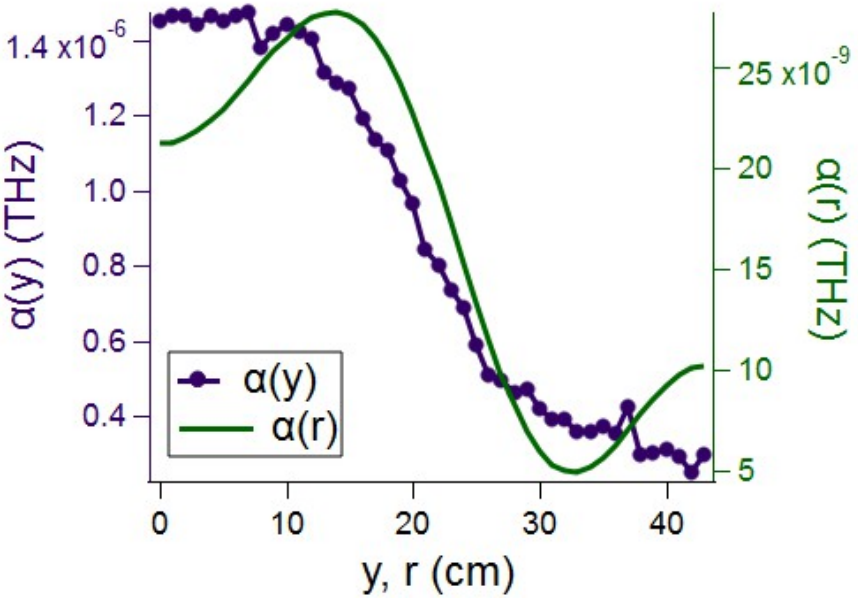

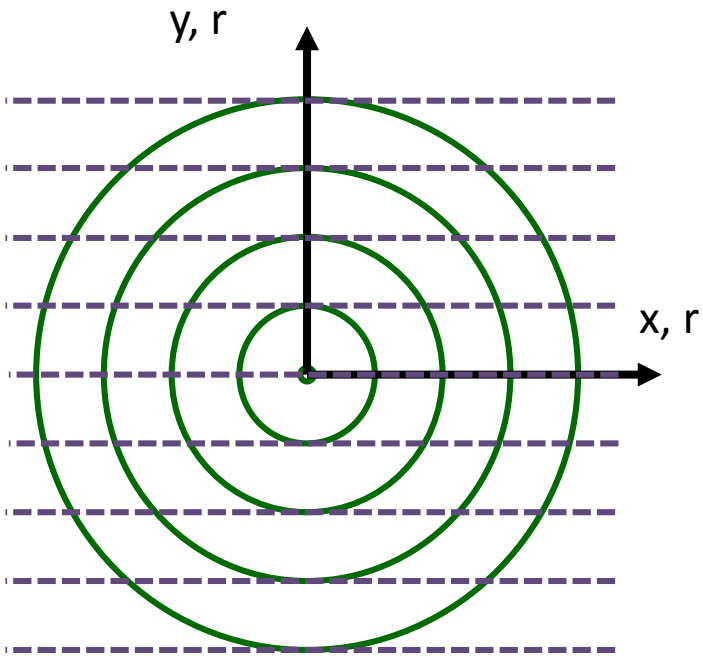

[11,12]

Inverse Abel Transform

- **Isentropic calculations predict core temperature of 353K at outlet**
  - Results are 1mm downstream of outlet
  - Magnitude of temperature drop agrees with Naik et al. (2009) and Woodmansee et al. (2004)
- **Transverse temperature trends are consistent with Woodmansee et al. (2004)**
  - Exit plane temperature measurements
- **Lower temperature regions coincide with edges of nozzle**

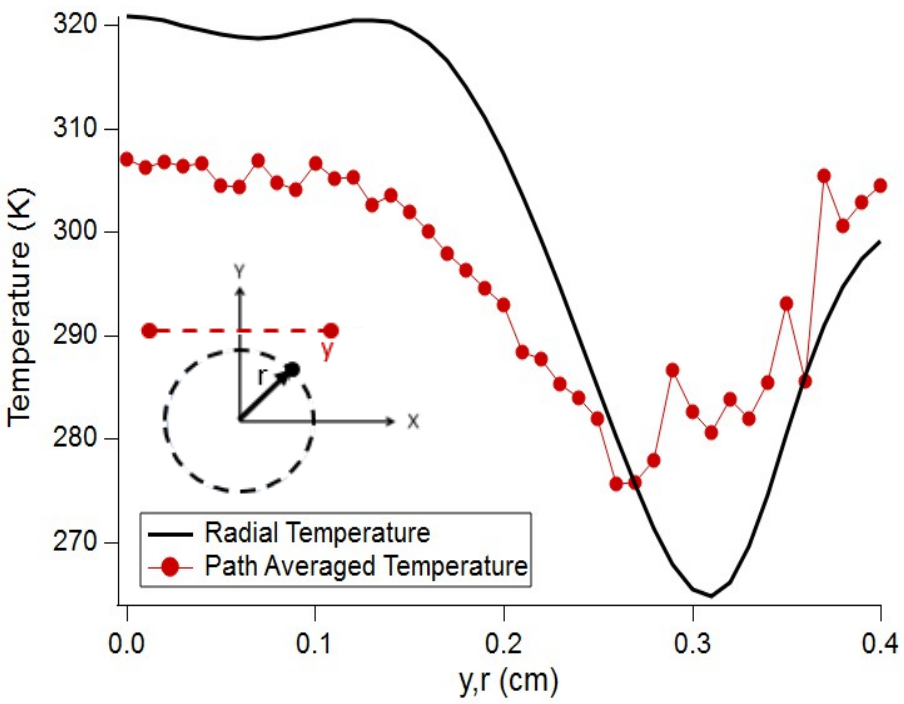

[11,12]

Species Concentration

- **Traditionally to calculate concentration (X) from absorbance area we must know pressure and path length**
  - Pressure distribution is unknown at measurement location
  - Edges of the plume are not distinctly defined

$$\alpha(\lambda) = S(T)PXL\Phi$$

- **Computational models could be used**
  - Time intensive
  - Could introduce large errors if not correct

- **Simulating pressure distributions adds complexity to absorbance area simulation**

Species Concentration

- **New technique similar to the temperature measurement technique shown earlier**
  - Take the ratio of absorbance areas of the NH_3 feature and the 1388 nm H_2O feature

$$\frac{A_{1388}}{A_{1527}} = \frac{S_{1388}(T)X_{H2O}\cancel{LP_{total}}}{S_{1527}(T)X_{NH3}\cancel{LP_{total}}} = \frac{S_{1388}(T)X_{H2O}}{S_{1527}(T)X_{NH3}} \qquad (1)$$

  - Assume NH_3 and H_2O are the only significant species

$$\sum_{i=1}^{N} X_i = 1 \rightarrow X_{NH3} + X_{H2O} = 1 \qquad (2)$$

  - Solve for X_{NH3} by combining Equation 1 and 2

$$X_{NH3} = \frac{S_{1388}(T)A_{1527}}{A_{1388}S_{1527}(T) + A_{1527}S_{1388}(T)}$$

Species Concentration

- **Mean mole fractions from data**
  - X_{H2O} = 0.167±0.013, X_{NH3} = 0.833±0.013 (dashed lines)
- **Expected mole fractions based on measured flow rates**
  - X_{H2O} = 0.172, X_{NH3} = 0.828 (solid lines)
- **Uncertainty on edges due to temperature uncertainty in *S(T)***

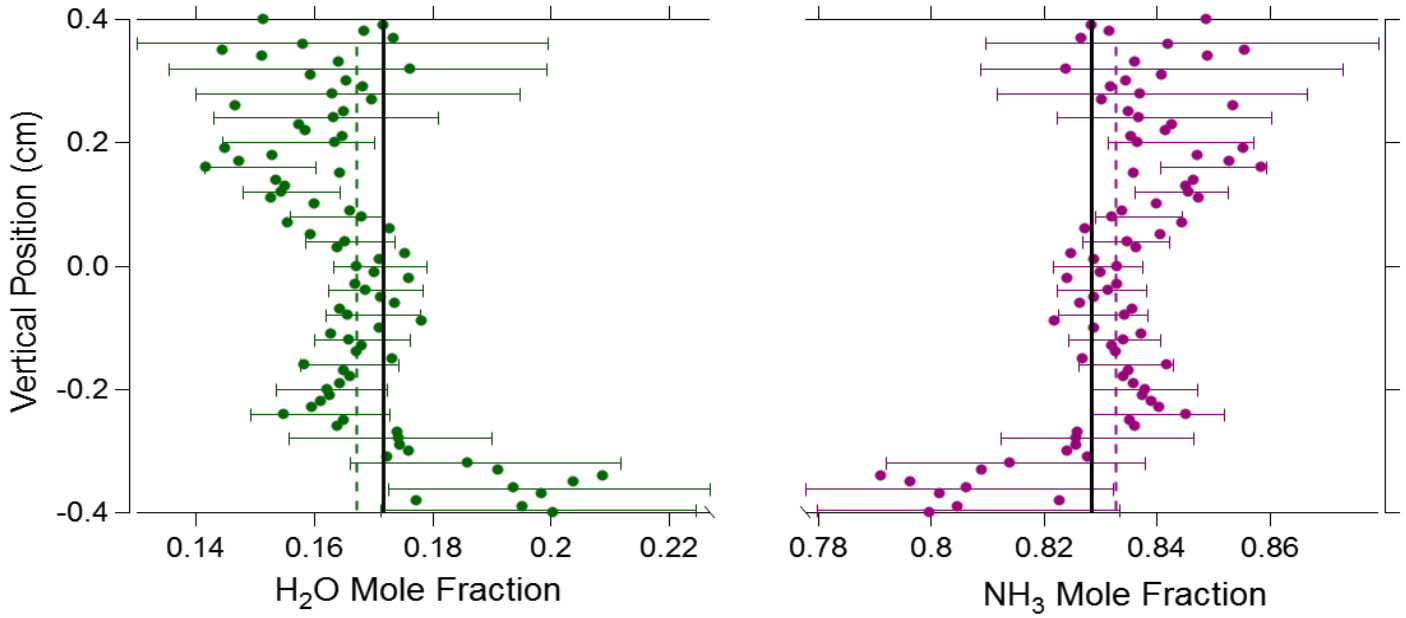

WMS as a Diagnostic

Benefits:

- **Small robust system**
- **Relatively inexpensive**
- **Easy alignment**
- **Calibration free**
- **Measurements of temperature and mole fraction**
- **Low power**
- **Fast acquisition times**
- **Non-intrusive**

Drawbacks:

- **Path averaged 1D measurements**
- **Velocity measurements are challenging**

WMS as a Diagnostic

Benefits:

- **Small robust system**
- **Relatively inexpensive**
- **Easy alignment**
- **Calibration free**
- **Measurements of temperature and mole fraction**
- **Low power**
- **Fast acquisition times**
- **Non-intrusive**

Drawbacks:

- **Path averaged 1D measurements**
- **Velocity measurements are challenging**

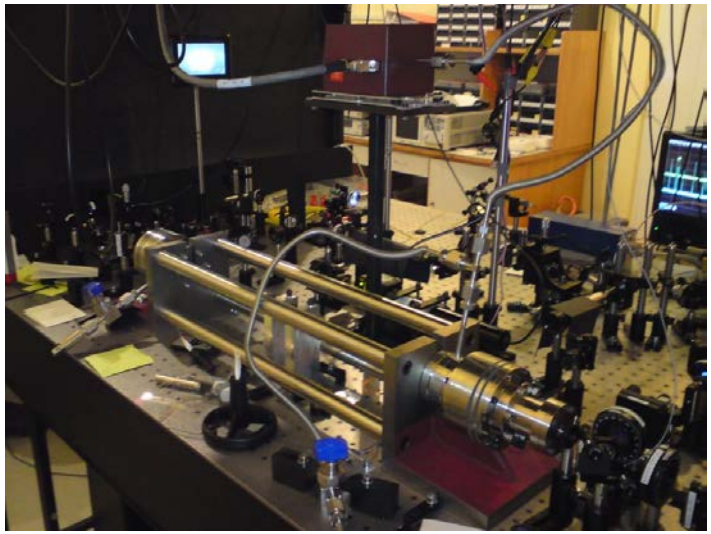

Cavity Ring Down Spectroscopy (CRDS)

http://ocmqs.fizyka.umk.pl/?q=node/12

WMS as a Diagnostic

Benefits:

- **Small robust system**
- **Relatively inexpensive**
- **Easy alignment**
- **Calibration free**
- **Measurements of temperature and mole fraction**
- **Low power**
- **Fast acquisition times**
- **Non-intrusive**

Drawbacks:

- **Path averaged 1D measurements**
- **Velocity measurements are challenging**

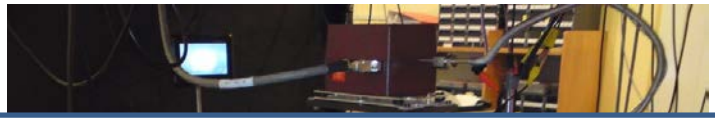

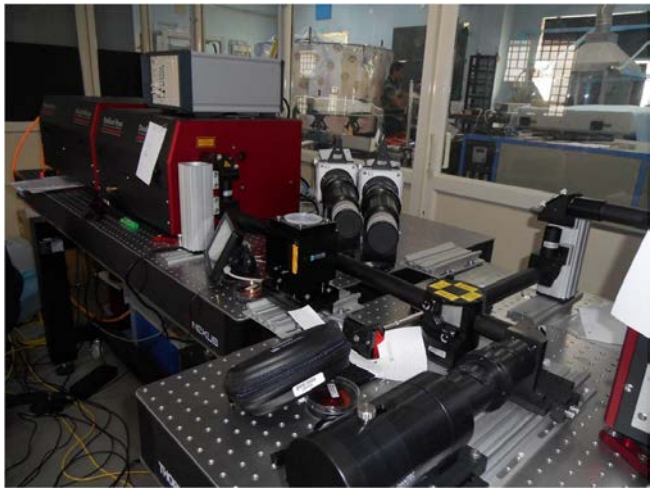

Planar Laser Induced Fluorescence (PLIF)

http://nccrd.in/facilities/equipment/19

WMS as a Diagnostic

Benefits:

- **Small robust system**
- **Relatively inexpensive**
- **Easy alignment**
- **Calibration free**
- **Measurements of temperature and mole fraction**
- **Low power**
- **Fast acquisition times**
- **Non-intrusive**

Drawbacks:

- **Path averaged 1D measurements**
- **Velocity measurements are challenging**

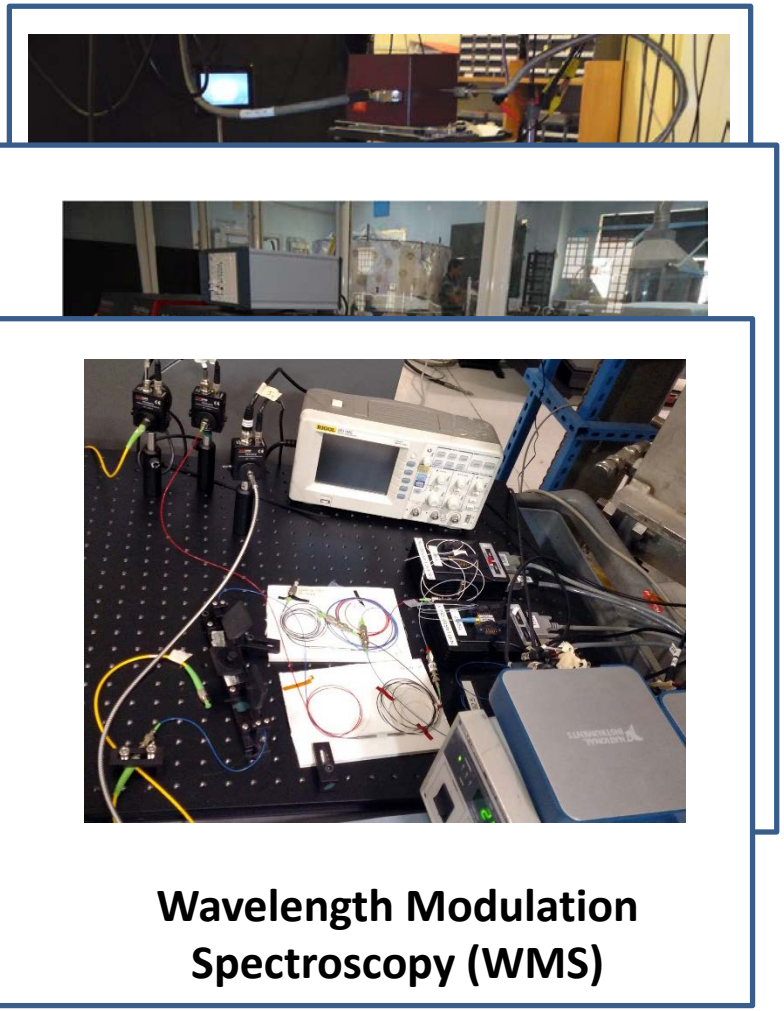

Wavelength Modulation Spectroscopy (WMS)

Conclusions and Acknowledgements

Conclusions:

- **Spatial distributions of temperature were calculated within the plume**
- **Radial temperature distributions were calculated using Abel inversions**
  - Temperature distributions consistent with previous experimental results [13,14]
- **New method for calculating species concentration was proposed**
  - Concentration measurements compare well with expected results
- **Results indicate WMS is a promising technique for microthruster diagnostics**

Acknowledgements:

The University of Colorado authors were supported under contract ROS151366C from Jacobs Technologies

University of Colorado:
Torrey Hayden
Dr. Greg Rieker
Precision Laser Diagnostic Laboratory

AFRL Collaborators:
Michael Nakles
Nickolas Pilgram
Dr. Natalia MacDonald
Dr. William Hargus

References

1. *NASA Seeks Proposals For Green Propellant Technology Demonstrations*. AmericaSpace. http://www.americaspace.com/?p=13617. (Feb 2012).
2. *19.3 A Molecular Interpretation of Entropy*. Chapter 19, Section 3. http://wps.prenhall.com/wps/media/objects/3083/3157971/blb1903.html
3. Rothman, L.S., et al., *The HITRAN2012 molecular spectroscopic database*, J. Quant. Spectrosc. Radiat. Transf., vol. 130, pp. 4–50, (Nov 2013).
4. Webber, M.E., *Diode Laser Measurements of NH3 and CO2 for Combustion and Bioreactor Applications*, Stanford University, (Jan 2001).
5. Goldenstein, C.S., and Hanson, R.K., *Diode-laser measurements of linestrength and temperature-dependent lineshape parameters for H2O transitions near 1.4 μm using Voigt, Rautian, Galatry, and speed-dependent Voigt profiles*, J. Quant. Spectrosc. Radiat. Transf., vol. 152, pp. 127–139, (Feb 2015).
6. Rieker, G.B. *Wavelength modulation spectroscopy for measurements of gas temperature and concentration in harsh environments*, Stanford University, (May 2009).
7. Rieker, G.B., Jeffries, J.B. and Hanson, R.K., *Calibration-free wavelength-modulation spectroscopy for measurements of gas temperature and concentration in harsh environments*, Appl. Opt., vol. 48, no. 29, p. 5546, (Oct 2009).
8. Sun, K., Chao, X., Sur, R., Goldenstein, C.S., Jeffries, J.B., and Hanson, R.K., *Analysis of calibration-free wavelength-scanned wavelength modulation spectroscopy for practical gas sensing using tunable diode lasers*, Meas. Sci. Technol., vol. 24, no. 12, p. 125203, (Dec 2013).
9. Goldenstein, C.S., Strand, C.L., Schultz, I.A., Sun, K., Jeffries, J.B., and Hanson, R.K., *Fitting of calibration-free scanned-wavelength-modulation spectroscopy spectra for determination of gas properties and absorption lineshapes*, Appl. Opt., vol. 53, no. 3, p. 356, (Jan 2014).
10. Hanson, R.K. and Falcone, P.K., *Temperature measurement technique for high-temperature gases using a tunable diode laser*, Appl. Opt., vol. 17, no. 16, p. 2477, (Aug 1978).
11. Liu, C., Xu, L., Li, F., Cao, Z., Tsekenis, S. A., and McCann, H., *Resolution-doubled one-dimensional wavelength modulation spectroscopy tomography for flame flatness validation of a flat-flame burner*, Appl. Phys. B, vol. 120, no. 3, pp. 407–416, (Jun 2015).
12. Matlock, T. S., Larson, C. W., Hargus Jr, W. A., and Nakles, M. R. *An Inversion Method for Reconstructing Hall Thruster Plume Parameters from Line Integrated Measurements*. 43rd AIAA/ASME/SAE/ASEE Joint Propulsion Conference and Exhibit, Cincinnati, OH. (2007).
13. M. A. Woodmansee, V. Iyer, J. C. Dutton, and R. P. Lucht, “Nonintrusive pressure and temperature measurements in an underexpanded sonic jet flowfield,” AIAA J., vol. 42, no. 6, pp. 1170–1180, 2004.
14. S. V. Naik, W. D. Kulatilaka, K. K. Venkatesan, and R. P. Lucht, “Pressure, Temperature, and Velocity Measurements in Underexpanded Jets Using Laser-Induced Fluorescence Imaging,” in AIAA journal, 2009, vol. 47, pp. 839–849.

Questions?

Data Processing

Water absorption features

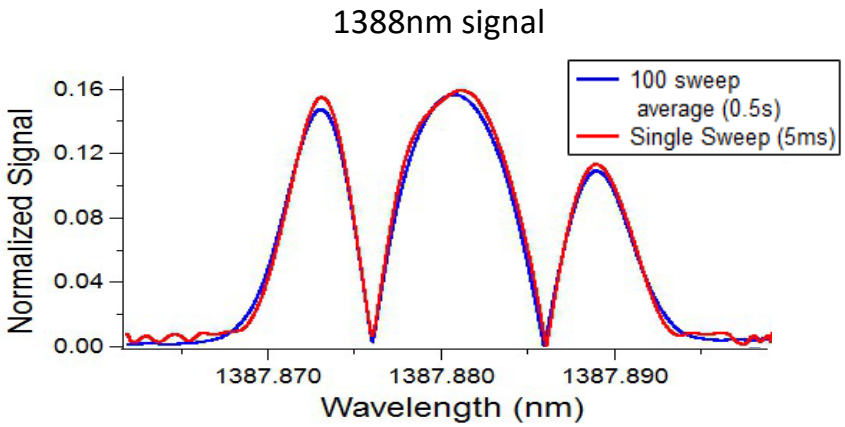

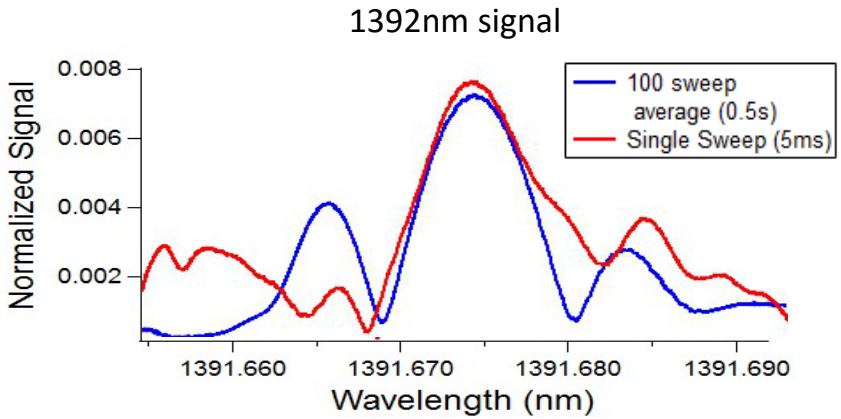

NH_3 absorption feature

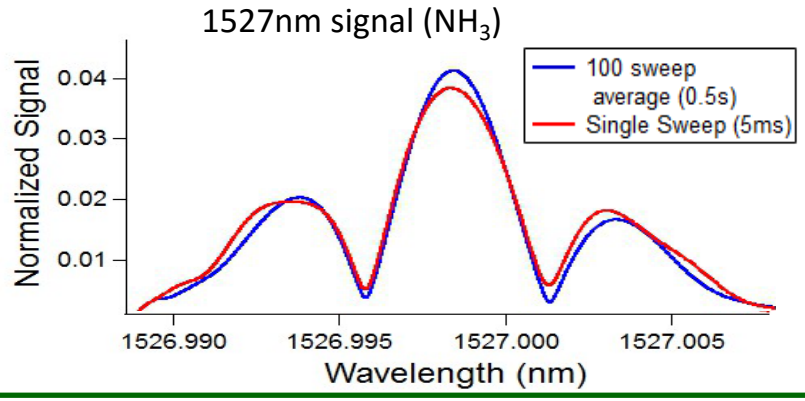

Data sets were averaged for 0.5 seconds to increase signal to noise ratio (SNR)

Residual Amplitude Modulation (RAM)

- **Non-linearity in the laser 2 was substantial**
- **I_o signal was used for background subtraction to account for this**

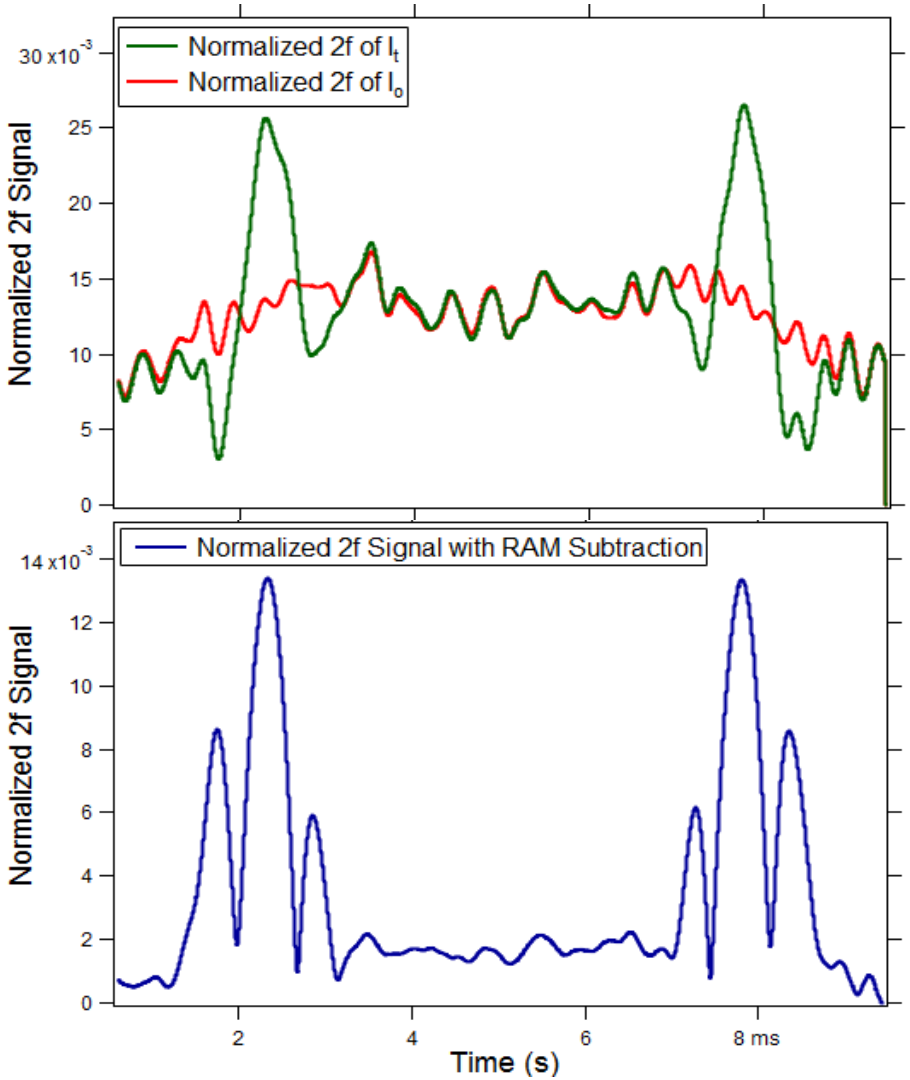

Wavelength Modulation Spectroscopy

X Component: $A\sin(fx+\phi)\cos(fx) = \frac{A}{2}\big(\sin(\phi)+\sin(2fx+b)\big)$

Y Component: $A\sin(fx+\phi)\sin(fx) = \frac{A}{2}\big(\cos(\phi)-\cos(2fx+b)\big)$

Magnitude: $\sqrt{\left(\frac{A}{2}\sin(\phi)\right)^2+\left(\frac{A}{2}\cos(\phi)\right)^2} = A/2$

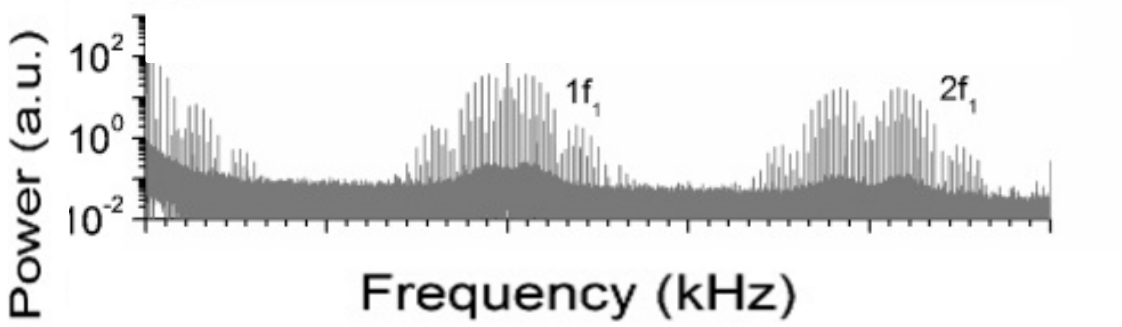

Data Processing

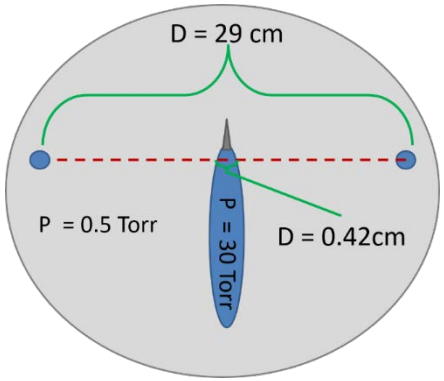

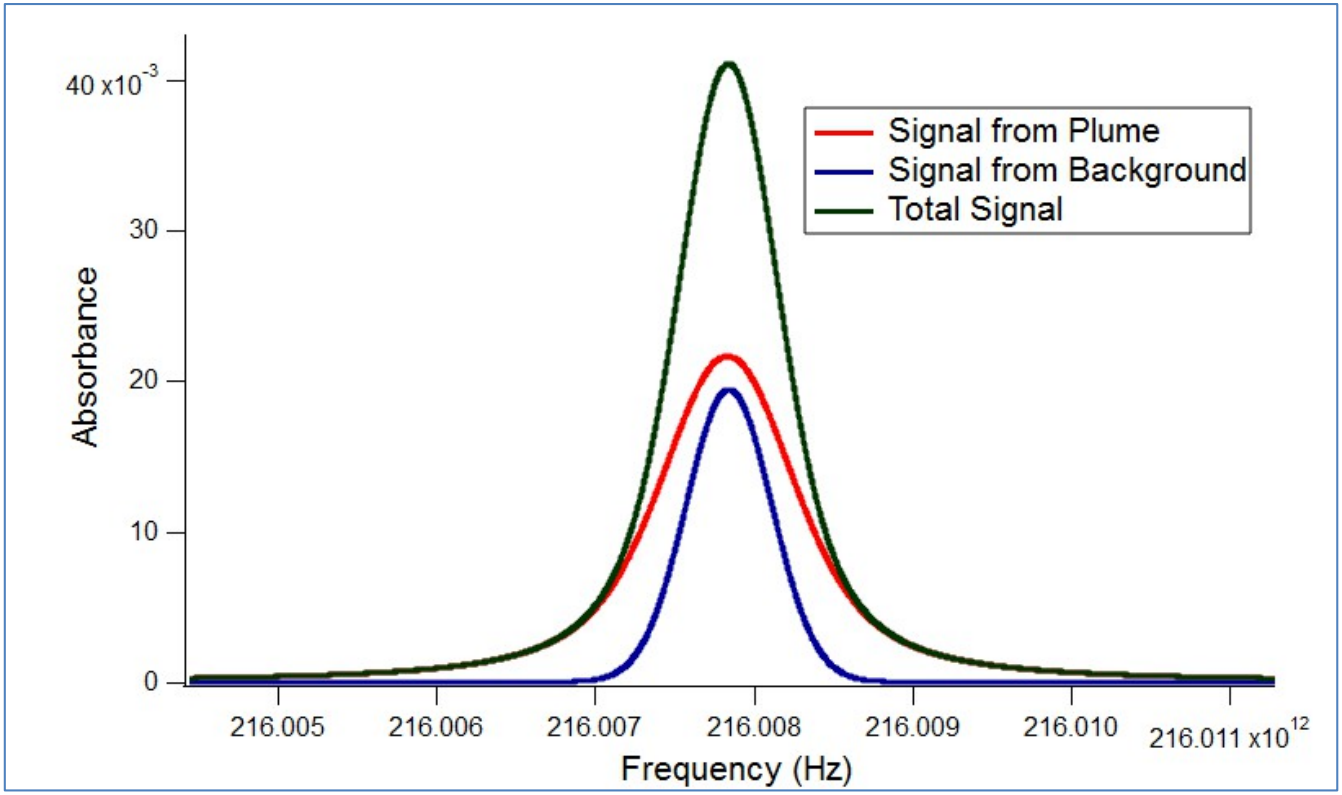

Inverse Abel Transform